The Energy-Cycle Analysis of the Interactions Between Shallow and Deep Atmospheric Convection

Robert S. Plant[a,*], Jun-Ichi Yano[b]

[a] *Department of Meteorology, University of Reading, UK*
[b] *GAME/CNRM, Météo-France and CNRS, 31057 Toulouse Cedex, France*

Abstract

Interactions between different convection modes can be investigated under the framework of an energy–cycle description. The present paper systematically investigates this system by taking a limit of two modes: shallow and deep convection. Shallow convection destabilizes itself as well as the other convective modes by moistening and cooling the environment, whereas deep convection stabilizes itself as well as the other modes by drying and warming the environment. As a result, shallow convection leads to a runaway growth process in its stand–alone mode, whereas deep convection simply damps out. Interaction between these two convective modes become a rich problem, even when it is limited to the case with no large–scale forcing, because of these opposing tendencies. Only if the two modes are coupled at an proper level can a self–sustaining system arise, exhibiting a periodic cycle. The main purpose of the present study is to establish the precise conditions for self–sustaining periodic solutions. It carefully documents the behaviour of the

*Correspondence address: Meteorology Department, University of Reading, RG6 6BB, UK

Email address: r.s.plant@reading.ac.uk (Robert S. Plant)

two mode system in order to facilitate the interpretation of global model behaviours when this energy–cycle is implemented as a closure into a convection parameterization in future.
Keywords: Parameterization, Closure, Convective–convective interactions, Transformation of shallow to deep convection

---

1. Introduction

The energy–cycle description of a convective system provides a basis for studying various dynamical behaviours of convective ensembles. The most formal manner for developing a convection parameterization is, in turn, to introduce a spectrum of convective types with various characteristic depths, as considered by Arakawa and Schubert (1974). Such a spectrum of convection types, and the interactions between the types, can best be described under the energy cycle framework.

Indeed, an energy cycle description for mass–flux convection parameterization was introduced in the seminal work by Arakawa and Schubert (1974), as presented by their Eqs. (132) and (142). Although the quasi–equilibrium situation has received much attention (Yano and Plant 2012c), relatively little attention has been paid to the full dynamical system so far, apart from a brief attempt by Randall and Pan (1993), Pan and Randall (1998) for taking this system as a basis of a prognostic parameterization closure. Recently, Yano and Plant (2012a, b) took up this system and showed that it can explain various basic convective processes in a rather lucid manner.

More precisely, Yano and Plant (2012a) showed that the basic mechanism driving a life cycle of discharge and recharge can be understood by a single

mode version (*i.e.*, deep convection only) of this system. Yano and Plant (2012b) demonstrated that such cycles could also occur in a two–mode system consisting of shallow and deep convection. The present study extends the latter, and performs a more comprehensive investigation of the two–mode system.

The chief aim of the present paper is, by presenting a systematic analysis, to more emphatically argue for the importance and possible impacts of explicitly considering the mutual interactions between shallow and deep convection in operational convection parameterization, which we previously merely suggested (Yano and Plant 2012b).

1.1. Types of convection: Background

Understanding the interactions between various types of convection is a basic motivation of the present study. As was emphasized in a review by Stevens (2005), "moist convection is not one, but many things". According to this review, atmospheric moist convection can be classified into three major categories. In order of increasing vertical extent these are stratocumulus, trade–wind cumulus, and deep precipitating cumulus convection. These major categories may also be considered as a series of transformations of the dominant mode of convection with an increasing supply of moisture from the surface under a horizontally homogeneous environment. Phenomenologically, such transformations are found as we move from the mid-latitudes to the warmer tropical oceans.

Here, by "horizontally homogeneous environment" we mean an idealized situation in which horizontal advection effects can be neglected. This is a useful idealization because convection is a process primarily concerned with

vertical transports. In the present study, such an idealization is adopted under the framework of a zero–spatial–dimension model.

Under this idealization, when moisture supply from the surface is totally absent, a constant heat supply from the surface (the sensible heat flux) tends to produce a well-mixed convective boundary layer. As surface moisture supply is increasingly supplied to such a system, above a threshold cloud is formed at the top of the boundary layer. Such cloud is typically stratiform, and the associated convection is called stratocumulus convection (*cf.*, Moeng 1998). As the surface moisture supply is further increased, there is a regime transition from stratiform clouds into "shallow" cumulus convective towers. This regime is called trade–cumulus convection (*cf.*, Riehl 1951, Betts 1997), because it is typically found over the trade–wind region in the sub-tropics. As the surface moisture supply increases still further (as we approach closer the equator), then a final regime transition occurs in which deep cumulus convection is realized, which may reach as high as the tropopause (*cf.*, Riehl and Malkus 1958, Houze and Betts 1981, Redelsperger 1997). This last transition from shallow to deep convection is considered relatively sharp, although the existence of middle–level clouds called "cumulus congestus" has been emphasized more recently (Johnson *et al.* 1999, Tung *et al.* 1999).

A major challenge in global atmospheric modelling is to represent these rich varieties of moist convection, and the transitions between them, by means of parameterizations. Currently no single unified parameterization exists, but rather each different type of convection is dealt using a different parameterization scheme. Typically, convection parameterization schemes are distinguished into shallow and deep versions in order to deal with trade

and deep cumulus convection separately (*e.g.*, Tiedtke, 1989). Stratocumulus clouds are often dealt with by a boundary–layer parameterization (*e.g.*, Holtslag and Boville 1993, Lock 1998, Lock *et al.* 2000), often also in combination with microphysics and stratiform cloud schemes (*cf.*, Wyant *et al.* 2007). The combination of these independently–developed schemes often causes a problem in simulating stratocumulus convection (*cf.*, Köller *et al.* 2011) and shallow/deep transitions (*e.g.*, Bechtold *et al.* 2004, Guichard *et al.* 2004, Grabowski *et al.* 2006).

A recent trend has seen some attempts to use a combination of eddy diffusion and mass flux approaches (*e.g.*, Neggers *et al.* 2009, Köller *et al.* 2011), especially for dealing with stratiform convection consistently with the other types of convection. Other significant recent efforts include attempts to generalize shallow–convection mass–flux parameterizations for deep convection (Hohenegger and Bretherton 2011, Mapes and Meale 2011).

The main claim of the present paper is that the energy–cycle description of convection can provide a lucid framework for representing those various types of convection in a more unified manner.

1.2. Truncation into two modes

The present study is based on the energy–cycle description for a spectrum of convection types under a mass–flux formulation. The spectral approach, originally developed by Arakawa and Schubert (1974), treats different convection types by different prescribed vertical structures. Although Arakawa and Schubert (1974) more specifically assumed an ensemble of entraining plumes in defining their vertical structures, we do not consider this as an essential feature of their formulation because other models for defining the

vertical mass flux structure could straightforwardly be incorporated into the general framework, as discussed in Yano and Plant (2012c).

Note that these various types of convection can loosely be categorized into two major types: "non-precipitating" shallow convection and precipitating deep convection. In doing so, we effectively consider stratocumulus and trade–cumulus convection together as being the first major type. Thus, in the present paper, we truncate a spectral representation of convection into only two modes: shallow and deep convection. The main reason for such a severe truncation is in order to elucidate the interactions between types in the simplest possible setting.

In the above, we added quotation marks to "non-precipitating" because shallow convection is rarely non-precipitating in a strict sense, although the precipitation is much weaker than that typical of deep convection. In fact, from the energy-cycle perspective, the fundamental separation between the two types is not whether the clouds are shallow or deep, but rather whether or not the precipiation is strong enough to alter the character of the thermodynamic budget. The key aspect is that the budgets for the two major convective types are qualitatively different.

In the shallow–convection regime, the main effects of convection on its environment are cooling and moistening. These tendencies are usually balanced by large–scale subsidence that warms and dries the environment. It is important to recognize that in the absence of such subsidence then the shallow–convective regime is self–destabilizing. Shallow convection moistens the environment because it is either non-precipitating or only weakly precipitating, and thus the condensed water must ultimately return to the

environment. The condensed water typically evaporates as soon as it detrains into the environment, leading to cooling as a result.

On the other hand, in the deep–convective regime, the main effects of convection on its environment are warming and drying. These tendencies are usually balanced by a large–scale ascent that cools and moistens the environment. It is important to recognize that in the absence of such ascent the deep–convective regime is self–stabilizing. Deep convection dries the environment because condensation within deep convection acts as a sink for moisture, which mostly returns to the surface by precipitation. The detrained dry air from deep convection must descend towards the surface as a return flow, associated with adiabatic warming.

1.3. Goals of the present paper

First, we will show that these two qualitatively different behaviours of convection can be easily incorporated and well described using an energy cycle. Second, we will show that the energy–cycle formulation can describe the interactions between shallow and deep convection. We emphasize that the latter aspect is somewhat neglected in current operational modelling configurations. Here we systematically investigate the behaviour of the coupled shallow–deep convective system, pointing out the importance of these interactions for operational modelling contexts. Note that an earlier implementation by Randall and Pan (1993), and Pan and Randall (1998) does not take account of these interaction effects.

Clearly our next major goal is to implement this fully–interactive system into an operational convection parameterization as a closure. In order to achieve this, the basic behaviour of the two–mode interacting system must

be carefully documented theoretically, in order to facilitate proper interpretations of the obtained behaviours under a global model implementation.

A key feature of the two–mode system is that it self–sustains with a perpetual periodic cycle if the opposing tendencies of shallow and deep convection are carefully balanced. The major effort of the present paper is spent on establishing the precise conditions for achieving this periodicity. Much of the following investigation assumes no large–scale forcing. As it turns out, even under such a drastic simplification, the system represents rich behaviours, which we systematically investigate.

1.4. Outline

The paper is organized as follows. The rationale for adopting the energy cycle is established in the next section by reviewing Arakawa and Schubert (1974). The formulation of the system is presented in Sec. 3. As it turns out, a major freedom of the present formulation is in choosing an exponent p introduced in Eq. (5) below. The cases with $p = 2$ and $p = 1$ are of particular physical interest and are systematically investigated in Secs. 4 and 5, respectively. The paper is concluded in Sec. 6.

2. Rationale

This section recalls some key ideas behind the energy–cycle formulation for the convective system, originally introduced by Arakawa and Schubert (1974), and carefully reproduced in Yano and Plant (2012a). The reader should bear in mind that although in the following we often call a convective type a plume for convenience, the convective types need not necessarily be defined by any particular plume model, but rather the types are distinguished

by vertical profiles fixed with time, whatever rule is invoked to determine the profiles.

Consider a system of N plume types and let the subscripts refer to the plume types. The convective kinetic energy K_i for type i evolves according to the following equation (Eq. 132, Arakawa and Schubert 1974):

$$\frac{dK_i}{dt} = A_i M_{bi} - D_i. \tag{2.0.1}$$

Thus, kinetic energy is generated from potential energy at a rate $A_i M_{bi}$, and lost at a rate D_i. The generation rate is proportional to the cloud-base mass flux M_{bi} and to the cloud work function A_i, which itself evolves as

$$\frac{dA_i}{dt} = F_i + \sum_j \mathcal{K}_{ij} M_{bj} \tag{2.0.2}$$

(Eq. 142, Arakawa and Schubert 1974). Here F_i is the large-scale forcing (radiative or advective tropospheric cooling, surface fluxes, etc) for convection. The action of convection itself on the cloud work function is described by the matrix $\mathcal{K}_{ij}$.

The two dominant physical processes described by the matrix $\mathcal{K}_{ij}$ are discussed in two paragraphs following Eq.(144) of Arakawa and Schubert (1974). The first process (see their Fig. 11) is adiabatic warming due to the compensative descent, $-M_j$, induced by a given convective plume j. This process reduces the cloud work function of all plume types. Mathematically speaking, this means that the interaction matrix cannot be treated as sparse: all cloud types influence all other cloud types. The second major process (see their Fig. 12) is cooling of the environment due to re–evaporation of detrained condensed (cloudy) air. This process increases the cloud work

function due to its destabilizing tendency, but it affects only the plumes of the same type or those reaching higher heights, because the effect occurs only at the detrainment level and so is not felt by shallower clouds.

Arakawa and Schubert (1974) argue that the second process (destabilization tendency) is always weaker than the first (stabilization). This argument is also consistent with arguments for convective damping put forth by Emanuel *et al.* (1994). However, our preliminary analysis based on Jordan's sounding suggests otherwise: elements of the $\mathcal{K}$ matrix can be positive (*i.e.*, destabilizing) when the precipitation efficiency of the convective cloud is weak. In that case, the cooling by re-evaporation of detrained cloud water is so strong that the given convective type self-enhances with time. It furthermore promotes the enhancement of convective plumes taller than the type in question.

The process is likely to contribute to tropospheric moistening after a dry intrusion, as observed, for example, during the TOGA-COARE period (Parsons *et al.* 2000). Shallow convective clouds are self-enhanced by destabilization of their environment through evaporative cooling of detrained cloud water. Thus the process assists the recovery from dry state to a more normal moist state.

Once deep convection begins to develop, it tends to stabilize the environmental state, and that contributes to suppression of shallower convective plumes. In this manner, this system described by a $\mathcal{K}$-matrix appears to reproduce a typical life cycle of the tropical convective system associated with the MJO. Benedict and Randall (2007) emphasize the importance of "localized destabilization via low-level warming and moistening" for the MJO.

Such a discharge–recharge cycle is analytically described by Yano and Plant (2012a) with the energy–cycle system.

3. Defining the system

3.1. System of equations

For a two-mode system the equations for the cloud work function, Eq. 2.0.2, read as follows (*cf.*, Yano and Plant 2012b):

$$\begin{aligned} \frac{dA_d}{dt} &= F_d - \gamma_d M_d + \beta_s M_s \\ \frac{dA_s}{dt} &= F_s + \gamma_s M_s - \beta_d M_d \quad . \end{aligned} \tag{3.1.1}$$

Here the subscripts s and d label shallow and deep convection, respectively. The β and γ parameters are elements of the $\mathcal{K}$ matrix, discussed in the last section, and are defined such that $\gamma_{s,d}$ denotes the effect of the labelled type of convection on the cloud work function for convection of that same type (*i.e.*, the diagonal matrix entries), whereas $\beta_{s,d}$ denotes the effect of the labelled type of convection on the cloud work function for convection of the other type (*i.e.*, the off-diagonal matrix entries). The equations have been written with signs chosen such that γ and β are expected to be positive from the physical arguments of the last section. Thus, we expect shallow convection to destabilize both shallow and deep convection, and we expect deep convection to stabilize both shallow and deep convection. Note also that the notation for the mass fluxes has been slightly simplified from Eq. 2.0.2. Henceforth we use M to denote the cloud–base values. Although Pan and Randall (1998) considered a similar system, they neglected the interactions between the convective modes by setting $\beta_{s,d} = 0$.

The equations for the convective kinetic energy, Eq. 2.0.1, read as follows

$$\begin{aligned} \frac{dK_d}{dt} &= M_d A_d - \frac{K_d}{\tau_d} \\ \frac{dK_s}{dt} &= M_s A_s - \frac{K_s}{\tau_s}. \end{aligned} \tag{3.1.2}$$

Here we have assumed that the dissipation D for each mode can be characterized in terms of $\tau_{s,d}$, a constant dissipation time scale.

In order to close the energy cycle of the convective system defined by Eqs. 3.1.1,3.1.2, we also introduce a functional relationship between the convective kinetic energy and the mass flux. This is given by

$$\begin{aligned} K_d &= \alpha_d M_d^p \\ K_s &= \alpha_s M_s^p \end{aligned} \tag{3.1.3}$$

with constants α_d, α_s and p.

In the following, we consider the cases of $p = 2$ and $p = 1$ in that order. Pan and Randall (1998) considered the case of $p = 2$, whereas Yano and Plant (2012a) focussed on the case of $p = 1$. Although cloud–resolving model studies as well as statistical theories (Emanuel and Bister 1996, Shutts and Gray 1999, Parodi and Emanuel 2009) clearly favour the case with $p = 1$ as reviewed in Yano and Plant (2012a), it is fair to say that the evidence is not overwhelming. Note that although the choice $p = 1$ may at first sight be objected to on dimensional grounds, this objection is not in fact substantiated, as discussed in Appendix A.

The two choices may be interpreted in terms of the assumed convective response to variations in the strength of the large-scale forcing. The choice $p = 1$ corresponds to an assumption that the response occurs mainly through

variations in the fractional area of convection, whereas $p = 2$ corresponds to an assumption that the response occurs mainly through variations of in-cloud vertical velocity. The analysis by Plant (2012) further argues that $p = 2$ may be appropriate if primary initiation mechanisms dominate whereas $p = 1$ may be appropriate if secondary initiation is important.

3.2. Estimate of physical parameters

An estimate for the cloud–work function consumption rate γ_d was presented by Yano and Plant (2012a). Specifically they argued that

$$\gamma_d \approx \int_{z_b}^{z_t} g \frac{\eta^2}{\rho T_0} \frac{\partial \overline{\theta}}{\partial z} dz \sim h \frac{g}{\rho_B T_0} \frac{\partial \overline{\theta}}{\partial z} \tag{3.2.1}$$

where z_b and z_t are cloud base and cloud top respectively, η is the vertical profile of mass flux after normalization by the cloud-base value, ρ is the density, T_0 a reference temperature and $\overline{\theta}$ the enviromental potential temperature. The vertical extent of convection is denoted as $h = z_t - z_b$. This expression assumes that the dominant contribution is warming induced by compensating descent, as discussed in Section 2. Yano and Plant (2012a) took the numerical values of $g \sim 10$ ms^{-2}, $h \sim 10^4$ m, $\rho \sim 1$ kgm^{-3}, $T_0 \sim 300$ K and $\partial \overline{\theta}/\partial z \sim 3 \times 10^{-3}$ Km^{-1} to obtain an order of magnitude estimate of 1 Jm^2 kg^{-2}. They further state that an explicit evaluation of the integral for an example profile suggested an additional factor of 2. We therefore take $\gamma_d = 2$ Jm^2 kg^{-2} here.

The effect of deep convection on the shallow convection work function is assumed to be dominated by the same physical process, and this leads to the estimate

$$\beta_d \approx \int_{z_b}^{z_{t,s}} g \frac{\eta_d \eta_s}{\rho T_0} \frac{\partial \overline{\theta}}{\partial z} dz \tag{3.2.2}$$

where z_t, s is the cloud top for shallow convection. The estimate is similar to that in Eq. 3.2.1, but there are numerical differences in that $h \sim 10^3$ m is a more suitable value for the vertical extent of shallow convection, and an explicit evaluation now suggests that a factor of ~ 1 arises from the normalized integral. Hence, we take $\beta_d = 0.1$ Jm^2 kg^{-2}.

The effects of shallow convection are described by the parameters γ_s and β_s and are expected to be dominated by the evaporation of detraining cloud condensate as argued in Section 2. Relevant expressions for this process are given in Eq. (B37) of Arakawa and Schubert (1974) but in their formulation is clearly rather sensitive to the value of the entrainment rate, and a detailed cloud model for shallow convection would be required in order to compute these parameters reliably. Some direct evaluations of the $\mathcal{K}$ matrix have been performed by JIY using a very simple cloud model similar to the entraining plume model of Arakawa and Schubert (1974). These evaluations suggest that $\gamma_s \sim \beta_d$ and $\beta_s \sim \gamma_d$ might be reasonable but it must be recognized that any estimates for γ_s and β_s are necessarily rather uncertain and possibly the parameters have an important case-to-case dependency. Motivated also by the fact that cases of particular physical interest arise for $\gamma_s/\beta_s = \beta_d/\gamma_d$ (as will be explained in the analysis below, in Section 4.4 especially), we take $\gamma_s = 0.1$ Jm^2 kg^{-2} and $\beta_s = 2$ Jm^2 kg^{-2} as being our default parameter choices.

There is little other information available in the literature on typical values for elements of $\mathcal{K}$. An exception is a very brief remark on p142 of Randall and Pan (1993) which states that a typical value for γ_s is of order 10 times smaller than that for γ_d. The estimates used here are certainly

consistent with that remark.

A typical value for the convective kinetic energy dissipation rate is also not well constrained theoretically (*cf.*, Yano and Plant, 2012a). However recent analysis of cloud–resolving modelling data by Cathy Hohenegger (2011, personal communication) suggests $\tau_s \sim \tau_d \sim 10^3$ s. Note that this estimate is not able to distinguish between shallow and deep convection, unfortunately.

The above parameters are required independently of the choice of p. In the next two subsections we discuss estimates of further parameters that are more specific to the cases of $p = 2$ and $p = 1$, respectively.

3.2.1. Estimate of physical parameters for the $p = 2$ case

In this case, the proportionality constant α appearing in Eq. 3.1.3 (with subscripts d and s to be added as required) is defined by

$$\alpha = \int_{z_b}^{z_t} \frac{\eta^2}{2\rho\sigma_c} dz \tag{3.2.3}$$

(*cf.*, Yano and Plant, 2012a). The notation has been already defined with the exception of σ_c, the fractional convective cloud area.

For the purposes of estimating an order of magnitude, we can write

$$\alpha \sim \frac{h}{\rho\sigma_c} \tag{3.2.4}$$

Taking h and ρ as estimated previously and $\sigma_c \sim 10^{-1}$ for both modes, we obtain $\alpha_d \sim 10^5$ m^4 kg^{-1} and $\alpha_s \sim 10^4$ m^4 kg^{-1}.

3.2.2. Estimate of physical parameters for the $p = 1$ case

In this case, the proportionality constant α appearing in Eq. 3.1.3 is defined by

$$\alpha = w_b \int_{z_b}^{z_t} \frac{\eta^2 \rho_b \sigma_b}{2\rho\sigma_c} dz \tag{3.2.5}$$

(Yano and Plant, 2012a). Here a subscript b has been introduced in order to denote quantities evaluated at cloud base. The α parameter may be estimated as

$$\alpha \sim h w_b \tag{3.2.6}$$

again with subscripts d and s to be added appropriately. Taking the same values for h as above, along with $w_b \sim 1$ ms^{-1} for both modes, we obtain $\alpha_d \sim 10^4$ m^2 s^{-1} and $\alpha_s \sim 10^3$ m^2 s^{-1}.

It is worth noting at this point that for the $p = 1$ case, stationary values for the cloud work functions can be determined directly from Eq. 3.1.2 using the parameters that have been presented. Denoting these stationary values with a subscript 0, they are

$$\begin{aligned} A_{d0} &= \frac{\alpha_d}{\tau_d} \sim \frac{10^4}{10^3} \sim 10 \text{ Jkg}^{-1} \\ A_{s0} &= \frac{\alpha_s}{\tau_s} \sim \frac{10^3}{10^3} \sim 1 \text{ Jkg}^{-1}. \end{aligned} \tag{3.2.7}$$

4. Analysis of the system: the $p = 2$ case

We consider the case of $p = 2$ first in this section, because the system becomes linear in this case as seen by Eqs. 4.0.8 and 4.0.9 below. This is in marked contrast to the nonlinear case of $p = 1$ to be considered in Section 5. Although we believe that $p = 1$ is more realistic than $p = 2$ (Section 3.1), it is nonetheless of interest to examine the two-mode system with $p = 2$. The linearity greatly facilitates the analysis while leaving the overall behaviour of the two-mode system qualitatively simliar. Thus, the analysis of the case with $p = 2$ provides some useful insights also for the case with $p = 1$.

Substitution of Eq. 3.1.3 with $p = 2$ into Eq. 3.1.2 gives

$$\begin{aligned} \dot{M}_d = & \frac{A_d}{2\alpha_d} - \frac{M_d}{2\tau_d} \\ \dot{M}_s = & \frac{A_s}{2\alpha_s} - \frac{M_s}{2\tau_s} \end{aligned} \tag{4.0.8}$$

while Eq. 3.1.1 is restated here as

$$\begin{aligned} \dot{A}_d = & -\gamma_d M_d + \beta_s M_s + F_d \\ \dot{A}_s = & \gamma_s M_s - \beta_d M_d + F_s \end{aligned} \tag{4.0.9}$$

We have introduced a dot in order to denote the time derivative. Eqs. 4.0.8 and 4.0.9 define the system with $p = 2$ as a set of four linear differential equations with constant coefficients.

In order to develop a feel for the coupled system, we first consider shallow and deep convection separately in Sections 4.1 and 4.2 respectively. We then turn to a special case of the coupled system in Section 4.3 in order to show some simplified examples of analytical solutions and numerical demonstrations. A more general analysis of the system is then presented in Sections 4.4 and 4.5. We continue in Section 4.6 with perturbation expansions about some limiting cases followed by an analysis of the conditions needed for a periodic solution in Section 4.7 and a summary of the $p = 2$ system in Section 4.8.

4.1. Shallow convection only

The equations for the shallow mode only are

$$\begin{aligned} \dot{M}_s = & \frac{A_s}{2\alpha_s} - \frac{M_s}{2\tau_s} \\ \dot{A}_s = & F_s + \gamma_s M_s \end{aligned} \tag{4.1.1}$$

and we neglect any large-scale forcing of shallow convection by setting $F_s = 0$.

Cloudy air is detrained from the top of shallow convection and re–evaporates as soon as it is detrained. This induces evaporative cooling, which further destabilizes the atmosphere. The re–evaporative cooling tendency dominates over the effects of diabatic warming by compensative descent for shallow convection, because it is only weakly precipitating. This is expressed by a positive value for γ_s, so that shallow convection increases the cloud work function, A_s. That increase in turn tends to increase the shallow convective mass flux, M_s, through the first term on the right hand side of the mass flux evolution equation.

Substituting a solution $M_s = M_s(0)e^{\sigma t}$ and $A_s = A_s(0)e^{\sigma t}$, we obtain

$$\sigma^2 + \frac{\sigma}{2\tau_s} - \frac{\gamma_s}{2\alpha_s} = 0 \tag{4.1.2}$$

so that

$$\sigma = -\frac{1}{4\tau_s} \pm \frac{1}{4\tau_s}\left(1 + \frac{8\tau_s}{\tau_{As}}\right)^{1/2} \tag{4.1.3}$$

where

$$\tau_{As} = (\alpha_s/\gamma_s)^{1/2} \sim 10^{5/2} \sim 300 \text{ s} \tag{4.1.4}$$

can be interpreted as a characteristic timescale associated with the shallow cloud work function.

Owing to the solution from the positive sign of the square root above, the shallow system is exponentially growing with time, regardless of the mass–flux damping timescale, τ_s. Thus the shallow-only system is self-destabilizing. An example integration is shown in Fig. 1.

With the inclusion of forcing it is straightforward to confirm that the

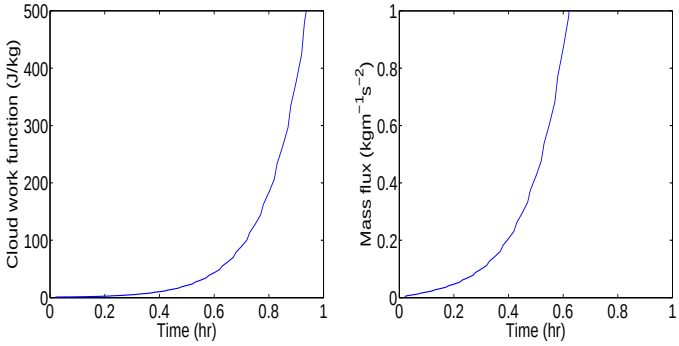

Figure 1: Example solution for the unforced shallow mode alone in the $p = 2$ system. The parameters are the default set described in Section 3.2. On the left and right respectively are shown the time series of the cloud work function and the mass flux.

eigenvalues are unaltered and the solution is shifted to

$$M_s = M_s(0)e^{\sigma t} - \frac{F_s}{\gamma_s}(1 - e^{\sigma t}) \tag{4.1.5a}$$

$$A_s = A_s(0)e^{\sigma t} - \frac{\alpha_s F_s}{\gamma_s \tau_s}(1 - e^{\sigma t}) \tag{4.1.5b}$$

thereby changing the details of the solution but not its basic character.

4.2. Deep convection only

The equations for the deep mode only are

$$\begin{aligned} \dot{M}_d = &\quad \frac{A_d}{2\alpha_d} - \frac{M_d}{2\tau_d} \\ \dot{A}_d = &\quad F_d - \gamma_d M_d \end{aligned} \tag{4.2.1}$$

again neglecting the large–scale forcing, $F_d = 0$.

Deep convection grows at a rate proportional to the cloud work function. However, the generated deep–convective mass flux consumes the cloud

work function, leading to the notion of convective damping (*cf.*, Emanuel *et al.* 1994).

Substituting a solution $M_d = M_d(0)e^{\sigma t}$ and $A_d = A_d(0)e^{\sigma t}$, we obtain

$$\sigma^2 + \frac{\sigma}{2\tau_d} + \frac{\gamma_d}{2\alpha_d} = 0 \tag{4.2.2}$$

so that

$$\sigma = -\frac{1}{4\tau_d} \pm \frac{1}{4\tau_d}\left(1 - \frac{8\tau_d}{\tau_{Ad}}\right)^{1/2} \tag{4.2.3}$$

where

$$\tau_{Ad} = (\alpha_d/\gamma_d)^{1/2} \sim (5 \times 10^4)^{1/2} \sim 200 \text{ s}. \tag{4.2.4}$$

The unforced deep convective system is always damping, regardless of the parameter choices. For $\tau_{Ad} > 8\tau_d$ there are two purely damping modes, whilst for $\tau_{Ad} < 8\tau_d$, the system exhibits a damping oscillations with a period of $8\pi\tau_d(8\tau_d/\tau_{Ad} - 1)^{-1/2}$. An example of a strongly damped oscillation is shown in Fig. 2, using the default parameters.

4.3. A special case: Mass flux equilibrates more quickly than work function

Henceforth we consider the full system in which shallow and deep convection are coupled. In the following Section 4.4 we consider the general case for any parameter set. Before doing so, it is instructive to consider a particular limit which provides some insight into how the coupled system can behave. Specifically, the present subsection considers a regime in which the mass flux evolution equations, Eq. 4.0.8, come into an equilibrium much more quickly than the cloud work function equations, Eq. 4.0.9. Such a situation arises when the kinetic energy dissipation timescales are much shorter than the cloud–work function timescales: *i.e.*, if

$$\tau_s \sim \tau_d \ll \tau_{As} \sim \tau_{Ad}. \tag{4.3.1}$$

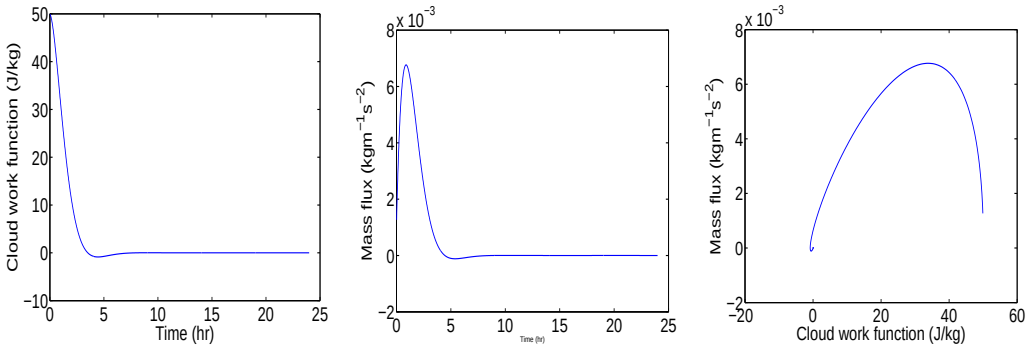

Figure 2: Example solution for the unforced deep mode alone in the $p = 2$ system. The parameters are the default set described in Section 3.2. From left to right are shown: the time series of the cloud work function, the time series of mass flux, and the trajectory in the phase space of the cloud work function (horizontal axis) and mass flux (vertical axis).

Taking the estimates from Sections 4.1 and 4.2, $\tau_{Ad} \sim 200$ s and $\tau_{As} \sim 300$ s, which is comparable with the default dissipation timescales $\tau_s = \tau_d = 10^3$ s. Thus the limit is unlikely to be a good approximation for most situations of physical interest, but it is nonetheless convenient for a conceptual demonstration.

Under this limit, Eq. 4.0.8 provides an approximate functional relationship between the cloud work functions and the mass fluxes,

$$\begin{aligned} A_d &\approx \frac{\alpha_d}{\tau_d} M_d \\ A_s &\approx \frac{\alpha_s}{\tau_s} M_s. \end{aligned} \tag{4.3.2}$$

Substitution of these relationships into Eq. 4.0.9 yields the relatively slow

evolution of the unforced cloud work functions as:

$$\begin{aligned} \dot{A}_d &= -\hat{\gamma}_d A_d + \hat{\beta}_s A_s \\ \dot{A}_s &= \hat{\gamma}_s A_s - \hat{\beta}_d A_d \end{aligned} \tag{4.3.3}$$

where we have introduced the notation

$$\begin{aligned} \hat{\gamma}_d &= \frac{\gamma_d \tau_d}{\alpha_d}, & \hat{\beta}_d &= \frac{\beta_d \tau_d}{\alpha_d}, \\ \hat{\gamma}_s &= \frac{\gamma_s \tau_s}{\alpha_s}, & \hat{\beta}_s &= \frac{\beta_s \tau_s}{\alpha_s}. \end{aligned} \tag{4.3.4}$$

Note that $\hat{\gamma}_d = \tau_d/\tau_{Ad}^2$ and $\hat{\gamma}_s = \tau_s/\tau_{As}^2$ are the slow rates at which the cloud work functions evolve.

Considering a solution of the form $\sim e^{\sigma t}$ results in the eigenfrequency equation

$$\sigma^2 + (\hat{\gamma}_d - \hat{\gamma}_s)\sigma - \hat{\gamma}_s\hat{\gamma}_d + \hat{\beta}_s\hat{\beta}_d = 0, \tag{4.3.5}$$

with solution

$$\sigma = \frac{1}{2}\left\{ \hat{\gamma}_s - \hat{\gamma}_d \pm \left[(\hat{\gamma}_s - \hat{\gamma}_d)^2 - 4(\hat{\beta}_s\hat{\beta}_d - \hat{\gamma}_s\hat{\gamma}_d) \right]^{1/2} \right\}. \tag{4.3.6}$$

Thus, we can have three types of solution:

(i) if $\hat{\gamma}_s > \hat{\gamma}_d$ then the solution grows (possibly a growing oscillation or possibly pure exponential growth);

(ii) if $\hat{\gamma}_s = \hat{\gamma}_d$ then the solution will be neutral if $\hat{\beta}_s\hat{\beta}_d = \hat{\gamma}_s\hat{\gamma}_d$, growing if $\hat{\beta}_s\hat{\beta}_d < \hat{\gamma}_s\hat{\gamma}_d$, or purely oscillatory if $\hat{\beta}_s\hat{\beta}_d > \hat{\gamma}_s\hat{\gamma}_d$;

(iii) if $\hat{\gamma}_s < \hat{\gamma}_d$ then the solution is damping with an oscillation if the argument of the square root is negative, pure damping if the argument of the square root is positive and if $\hat{\beta}_s\hat{\beta}_d > \hat{\gamma}_s\hat{\gamma}_d$, and growing if the argument of the square root is positive and if $\hat{\beta}_s\hat{\beta}_d < \hat{\gamma}_s\hat{\gamma}_d$.

Figs. 3, 4 and 5 give examples respectively of numerical solutions for a growing set of parameters with case (i), an oscillatory set of parameters with case (ii) and a damping set of parameters with case (iii). As noted above, the limiting case considered in this subsection is primarily of conceptual interest. To produce these figures we chose parameter values considerably removed from the default set of Section 3.2 in order to respect the limiting approximation. A consequence of the choices is that the cloud work functions and mass fluxes sometimes take negative values during the resulting evolution. Note also that each example exhibits a rapidly decaying transient for the mass flux over the first 2 hr before the longer time behaviour becomes apparent.

In physical terms, these limiting analytical results show that the system may be growing or damping depending on whether self–growing shallow convection ($\hat{\gamma}_s$) or self–damping deep convection ($\hat{\gamma}_d$) dominates respectively. However, if the destabilization and stabilization tendencies can be balanced then we can obtain a neutral state.

4.4. General case

We now proceed to consider the *general* case of the coupled $p = 2$ system, Eqs. 4.0.8 and 4.0.9, without approximation.

As a linear system of ordinary differential equations with constant coefficients it has a solution of the form $e^{\sigma t}$ for each of the dependent variables, and a quartic eigenfrequency equation for σ is easily derived. However, the obtained equation is not physically illuminating and not stated here.

The analysis of the special case in Section 4.3 reveals that the overall behaviour of the unforced coupled system is determined by a competition between the growing tendency of shallow convection and the damping ten-

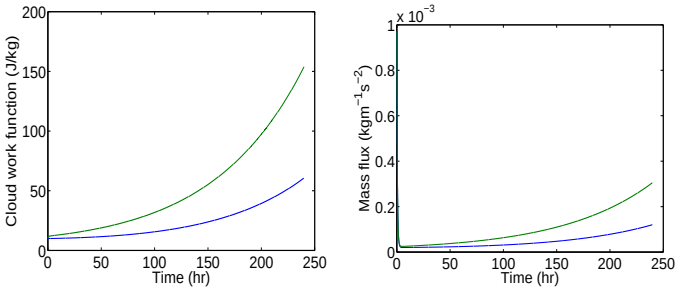

Figure 3: Example solution for the unforced $p = 2$ system with parameters chosen to illustrate case (i) of Section 4.3. Blue is for the deep mode and green for the shallow mode. The parameters are $\gamma_d = 1, \gamma_s = 2, \beta_d = \beta_s = 1$ Jm^2 kg^{-2}, $\alpha_d = \alpha_s = 5 \times 10^8$ m^4 kg^{-1} and $\tau_d = \tau_s = 10^3$ s, giving values of $\tau_{As} = 1.6 \times 10^5$ s and $\tau_{Ad} = 2.2 \times 10^5$ s. Shown in the same format as in Fig. 1.

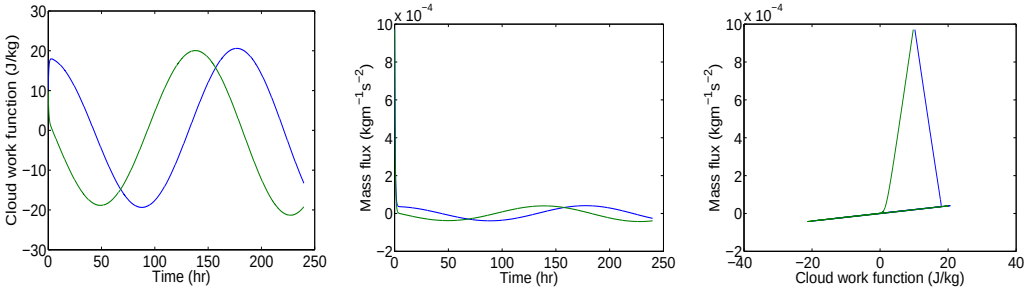

Figure 4: Example solution for the unforced $p = 2$ system with parameters chosen to illustrate case (ii) of Section 4.3. Blue is for the deep mode and green for the shallow mode. The parameters are $\gamma_d = \gamma_s = 1, \beta_d = \beta_s = 5$ Jm^2 kg^{-2}, $\alpha_d = \alpha_s = 5 \times 10^8$ m^4 kg^{-1} and $\tau_d = \tau_s = 10^3$ s, giving values of $\tau_{As} = \tau_{Ad} = 2.2 \times 10^5$ s. Shown in the same format as in Fig. 2.

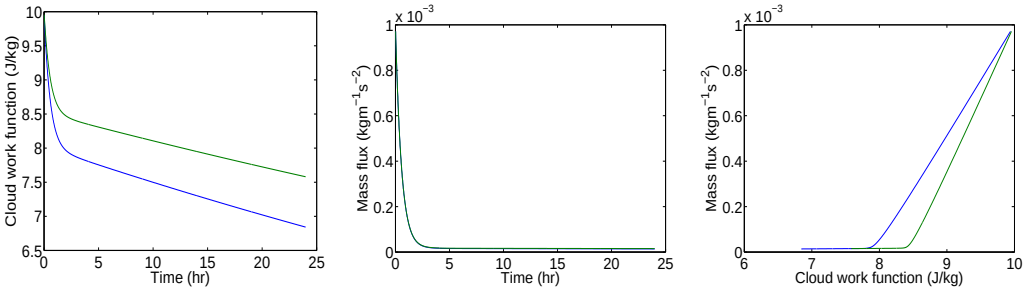

Figure 5: Example solution for the unforced $p = 2$ system with parameters chosen to illustrate case (iii) of Section 4.3. Blue is for the deep mode and green for the shallow mode. The parameters are $\gamma_d = 2, \gamma_s = 0.25, \beta_d = \beta_s = 1$ Jm^2 kg^{-2}, $\alpha_d = \alpha_s = 5 \times 10^8$ m^4 kg^{-1} and $\tau_d = \tau_s = 10^3$ s, giving values of $\tau_{As} = 1.6 \times 10^5$ s and $\tau_{Ad} = 4.5 \times 10^5$ s. Shown in the same format as in Fig. 2.

dency of deep convection. For most parameter choices, one of those tendencies is dominant and convection either explodes or dies out. However, there may be parameter settings that allow a balance to be realized between these two tendencies (*e.g.*, Fig. 4). A natural question to ask is under what conditions can we obtain such a balanced solution. It turns out that many of the same considerations arise for the nonlinear coupled system with $p = 1$ (Section 5.3).

4.4.1. The vanishing determinant

Consider the cloud work function tendency equations, Eq. 4.0.9, and look for a solution which is non-trivial in the absence of forcing. By non-trivial we mean a solution in which both M_s and M_d neither tend to zero nor tend to infinity, even for very long times. This is clearly a strong constraint on the problem. It is not physically reasonable to imagine that all of the environ-

mental parameters of a convective system (such as the $\mathcal{K}$ matrix elements) stay fixed in perpetuity, and so in practice we may be interested in cases where the coupled system does decay or grow, so long as that occurs relatively slowly. Nonetheless we will pursue this strict constraint, while bearing in mind that it is likely to lead us to overly restrictive constraints on the parameters.

A non-trivial solution in the above sense can be achieved if the solution becomes periodic so that A_s and A_d vary over time but they do so in such a way that their time-averaged variation vanishes over some finite period T. Setting the forcing to zero in Eq. 4.0.9 and denoting by an overbar the time average over period T then the solutions of interest occur for

$$\begin{aligned} -\gamma_d \overline{M_d} + \beta_s \overline{M_s} &= 0 \\ \gamma_s \overline{M_s} - \beta_d \overline{M_d} &= 0 \end{aligned} \tag{4.4.1}$$

so that

$$\beta_d \beta_s = \gamma_d \gamma_s. \tag{4.4.2}$$

In other words, the determinant of the $\mathcal{K}$ matrix must vanish for a non-trivial solution in the absence of forcing. For the remainder of Section 4 we will assume that this condition is indeed satisfied and examine the consequences.

There are several important remarks that should be made about this condition. First, note that the argument is easily extended to any number of convective modes. Second, note that the argument depends on the cloud work function tendency equations only. As such, the condition is entirely independent of the assumed functional form of the kinetic energy dissipation in Eq. 3.1.2 and of the assumed functional relationship between convective

kinetic energy and cloud base mass flux. In particular, it is independent of the choice of p. Third, we note that the set of default parameter choices discussed in Section 3.2 satisfies the condition. As alluded to earlier, this last point is not accidental, but it nonetheless does illustrate that the condition may be satisfied for physically–plausible parameter settings.

4.4.2. Linking the cloud work functions

We are now in a position to simplify the cloud work function tendency equations, Eq. 4.0.9. Expressing the unforced equation for shallow convection as

$$\dot{A}_s = \frac{\gamma_s}{\beta_s}\left(\beta_s M_s - \frac{\beta_d \beta_s}{\gamma_s} M_d\right) \tag{4.4.3}$$

and using Eq. 4.4.2 for the vanishing determinant, we have

$$\dot{A}_s = \frac{\gamma_s}{\beta_s}\left(\beta_s M_s - \gamma_d M_d\right). \tag{4.4.4}$$

Next we substitute for the term in brackets on the right-hand-side by using the tendency equation for the evolution of the deep cloud work function. This produces

$$\dot{A}_s = \frac{\gamma_s}{\beta_s}\dot{A}_d. \tag{4.4.5}$$

Hence (in the absence of forcing) the cloud work function tendencies are proportional for shallow and deep convection.

We can integrate the above equation to relate the two work functions directly,

$$A_s - A_s(0) = \frac{\gamma_s}{\beta_s}\left(A_d - A_d(0)\right). \tag{4.4.6}$$

This relationship is a simple consequence of the vanishing determinant and so applies with all the generality discussed in the previous subsection.

As a short aside on the forcing, note that if forcing were to be retained then the two work functions would be related by

$$A_s - A_s(0) = \frac{\gamma_s}{\beta_s}\left(A_d - A_d(0)\right) + \left(F_s - \frac{\gamma_s}{\beta_s}F_d\right)t \tag{4.4.7}$$

The term proportional to t clearly prevents a closed orbit solution in phase space. However, that term would vanish if

$$F_s = \frac{\gamma_s}{\beta_s}F_d. \tag{4.4.8}$$

This includes the case of zero forcing, but it is also interesting that forcing could be incorporated into all of the following analysis, if it were related by Eq. 4.4.8 for the two modes of convection.

4.5. The $p = 2$ equations with vanishing determinant: General considerations

Here we consider the unforced $p = 2$ system with a vanishing determinant but with no other constraints or approximations. Using Eq. 4.4.6 we can eliminate A_s in the prognostic equation 4.0.8 for M_s to yield:

$$\dot{M}_s = \frac{A_s(0)}{2\alpha_s} - \frac{\gamma_s A_d(0)}{2\alpha_s\beta_s} + \frac{\gamma_s}{2\alpha_s\beta_s}A_d - \frac{M_s}{\tau_s} \tag{4.5.1}$$

The above equation should be considered alongside those for the deep mode (Eqs. 4.0.8 and 4.0.9) which are restated here for convenience

$$\dot{M}_d = \frac{A_d}{2\alpha_d} - \frac{M_d}{2\tau_d} \tag{4.5.2}$$

$$\dot{A}_d = F_d - \gamma_d M_d + \beta_s M_s. \tag{4.5.3}$$

We try a solution of the following form

$$\begin{aligned} A_d &= A_d(0)e^{\sigma t} + a_0(1 - e^{\sigma t}) \\ M_d &= M_d(0)e^{\sigma t} + d_0(1 - e^{\sigma t}) \\ M_s &= M_s(0)e^{\sigma t} + s_0(1 - e^{\sigma t}) \quad , \end{aligned} \tag{4.5.4}$$

where the coefficients a_0, d_0 and s_0 can be obtained by substituting in the trial solution and then comparing the constant terms to give

$$\tau_d a_0 = \alpha_d d_0 \tag{4.5.5a}$$

$$\beta_s s_0 = \gamma_d d_0 \tag{4.5.5b}$$

$$\frac{s_0}{\tau_s} = \frac{\gamma_s}{\alpha_s \beta_s} d_0 + \frac{A_s(0)}{\alpha_s} - \frac{\gamma_s A_d(0)}{\alpha_s \beta_s}. \tag{4.5.5c}$$

The solution for a_0 is easily obtained,

$$a_0 = [\beta_s A_s(0) - \gamma_s A_d(0)] \left[\frac{\alpha_s \gamma_d \tau_d}{\alpha_d \tau_s} - \gamma_s \right]^{-1}, \tag{4.5.6}$$

whilst d_0 and s_0 are simply proportional to this, as given in Eqs. 4.5.5a and 4.5.5b respectively.

Comparing coefficients of the exponential terms that occur in the trial solution gives three equations in terms of a_0, d_0, s_0 and σ. These reduce to the eigenfrequency equation

$$\sigma^3 + \frac{\sigma^2}{2}\left(\frac{1}{\tau_d} + \frac{1}{\tau_s}\right) + \frac{\sigma}{4}\left[\frac{1}{\tau_d \tau_s} + 2\left(\frac{\hat{\gamma}_d}{\tau_d} - \frac{\hat{\gamma}_s}{\tau_s}\right)\right] + \frac{1}{4\tau_d \tau_s}(\hat{\gamma}_d - \hat{\gamma}_s) = 0 \tag{4.5.7}$$

which we have rewritten in terms of the rescaled self–interaction coefficients introduced in Eq. 4.3.4. Note that in terms of these rescaled coefficients the vanishing determinant condition reads

$$\hat{\beta}_d \hat{\beta}_s = \hat{\gamma}_d \hat{\gamma}_s. \tag{4.5.8}$$

An explicit formal solution can be written for the above eigenequation, but is not very illuminating. Nonetheless, we can offer some useful remarks. A cubic equation may have three real roots, or else one real root with one complex–conjugate pair. In order for the solution not to explode, we require

that any real roots are negative or zero, whereas any complex conjugate roots must have a negative real part. In either case, the product of the three roots must be negative or zero[1]. Since the product of the roots is given by minus the constant term in Eq. 4.5.7 it follows that to avoid an exploding solution

$$\hat{\gamma}_d \geq \hat{\gamma}_s \tag{4.5.9}$$

Physically this requirement is for the damping rate of the deep cloud work function, $\hat{\gamma}_d$, to exceed the generation rate of the shallow cloud work function, $\hat{\gamma}_s$.

A non-exploding case with three negative real roots will decay towards an equilibrium state with $A_d = a_0$, $M_d = d_0$, $M_s = s_0$, whilst a case with complex roots may be more interesting as pure imaginary roots decay towards a purely oscillating solution. It is possible to write down an explicit inequality in order for a cubic equation to have non-real roots, but again that is not physically illuminating and we cannot say from that whether those roots are explosive.

We close this subsection by remarking that the eigenequation 4.5.7 does not include $\hat{\beta}_s$ or $\hat{\beta}_d$. Thus, provided that these interaction coefficients are such as to produce a vanishing determiant their value does not otherwise affect the character of the solution.

[1]Moreover, the sum of roots must be negative. However, this is guaranteed since the coefficient of the quadratic term in Eq. 4.5.7 is positive definite.

4.6. The $p = 2$ equations with vanishing determinant: Perturbation approaches

In the previous subsection, we derived the cubic eigenequation 4.5.7 for the general case of the unforced $p = 2$ system with vanishing determinant. However, we noted that a formal solution to this equation is not physically instructive. Therefore, in the following subsections we specialize to situations where $\tau_s \approx \tau_d$ (Sections 4.6.1 and 4.6.2), where $\tau_s \ll \tau_d$ (Section 4.6.3) and where $\tau_s \gg \tau_d$ (Section 4.6.4), in order to illustrate the behaviour of the system in a more useful way. First we consider the case of $\tau_s = \tau_d$ in Section 4.6.1, and then in Section 4.6.2 we consider small departures from equality of the dissipation time scales, by means of a perturbation expansion.

The starting point for these analyses is to express the eigenequation in terms of the new variables

$$\begin{aligned} \xi_s &= \sigma(2\sigma\tau_s + 1) \\ \xi_d &= \sigma(2\sigma\tau_d + 1) \end{aligned} \tag{4.6.1}$$

in terms of which it reads

$$\xi_s\xi_d + \hat{\gamma}_d\xi_s - \hat{\gamma}_s\xi_d + (\hat{\beta}_s\hat{\beta}_d - \hat{\gamma}_s\hat{\gamma}_d) = 0. \tag{4.6.2}$$

This is the full quartic equation, which can easily be seen to reduce to a cubic if the term in brackets vanishes, as occurs for the vanishing determinant condition of Eq. 4.5.8.

4.6.1. The case of $\tau_s = \tau_d$

Assuming a vanishing determinant, and specializing also to the case of $\tau_s = \tau_d$ then we can work in terms of the variable $\xi = \xi_s = \xi_d = \sigma(2\sigma\tau + 1)$

where $\tau = \tau_s = \tau_d$. This variable satisfies the equation

$$\xi^2 + (\hat{\gamma}_d - \hat{\gamma}_s)\xi = 0 \tag{4.6.3}$$

leading to

$$\xi = 0 \quad \text{or} \quad \xi = \hat{\gamma}_s - \hat{\gamma}_d. \tag{4.6.4}$$

By solving the definition of ξ to obtain σ, we find that

$$\sigma = -\frac{1}{4\tau} \pm \left[\left(\frac{1}{4\tau} \right)^2 + \frac{\xi}{2\tau} \right]^{1/2} \tag{4.6.5}$$

so that the eigenfrequencies are:

$$\sigma = -\frac{1}{2\tau} \tag{4.6.6a}$$

$$\sigma = -\frac{1}{4\tau} \pm \left[\left(\frac{1}{4\tau} \right)^2 + \frac{1}{2\tau}(\hat{\gamma}_s - \hat{\gamma}_d) \right]^{1/2} \tag{4.6.6b}$$

Thus the characteristics of the system are determined by $\hat{\gamma}_s - \hat{\gamma}_d$. If $\hat{\gamma}_d < \hat{\gamma}_s$ and shallow convection dominates then then there is a growing solution without oscillation (the square root term produces a positive eigenfrequency when the square root is taken with a plus). If $\hat{\gamma}_s + 1/(8\tau) > \hat{\gamma}_d > \hat{\gamma}_s$ then deep convection is weakly dominant and there is a damping solution (the square root term is real but is not large enough in magnitude to be able to change the sign of σ). If $\hat{\gamma}_d > \hat{\gamma}_s + 1/(8\tau)$ then deep convection is more strongly dominant and there is a damping solution with an oscillation (the square root is imaginary).

We can of course solve the cubic eigenequation 4.5.7 numerically. Fig. 6 shows the phase diagram produced, which is easily checked to be consistent with the analysis just presented.

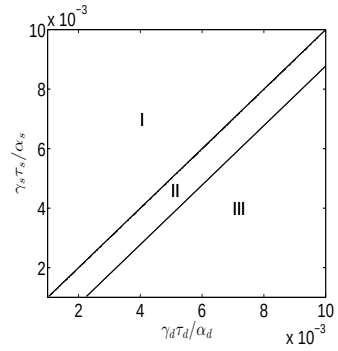

Figure 6: Numerically–generated phase diagram for the $p = 2$ system with vanishing determinant. The default parameters described in Section 3.2 are used for α_s and α_d, while a parameter choice for β_s and β_d is not required. The values for γ_s and γ_d have been varied to produce the diagram. The parameters τ_s and τ_d have been set to 10^2 s here rather than their default values of 10^3 s, in order to clarify the presence of region II, which is much thinner with the default values. Region I produces exploding cases ($\gamma_s > \gamma_d$), region II has pure decay cases ($\hat{\gamma}_s + 1/(8\tau) > \hat{\gamma}_d > \hat{\gamma}_s$) and region III has decay–with–oscillation cases ($\hat{\gamma}_d > \hat{\gamma}_s + 1/(8\tau)$). The regions are separated by plotting two contours for the eigenvalue with the largest real part. The contour where that real part is zero separates regions I and II. The contour where the imaginary part of that same eigenvalue is zero separates regions II and III.

It should be noticed there is no possibility for a purely imaginary (i.e., perpetually and stably periodic) solution. This is because any solution with an imaginary eigenvalue also has a negative real part for that eigenvalue. Or, in other words, because there is no imaginary part to the eigenvalue. There is no point of contact between regions I and III in the phase diagram.

To illustrate some particular cases taken from Fig. 6, Figs. 7, 8 and 9 give examples respectively of numerical solutions in regions: (I) a growing solution; (II) pure decay to constant values; and, (III) decay–with–oscillation.

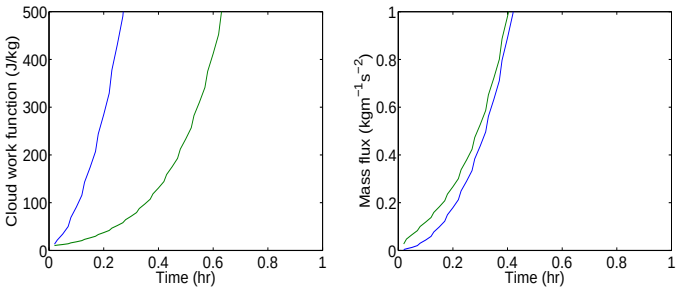

Figure 7: Example solution for the unforced $p = 2$ system with parameters chosen to illustrate region I of Fig. 6. Blue is for the deep mode and green for the shallow mode. The parameters are $\gamma_d = 2, \gamma_s = 0.4, \beta_d = 0.2, \beta_s = 4$ Jm^2 kg^{-2} and $\tau_d = \tau_s = 10^2$ s, together with the default choices for α_s and α_d described in Section 3.2. These choices give $\hat{\gamma}_s = 4 \times 10^{-3}$ s^{-1} and $\hat{\gamma}_d = 2 \times 10^{-3}$ s^{-1}, so that $\hat{\gamma}_s > \hat{\gamma}_d$. Shown in the same format as in Fig. 1.

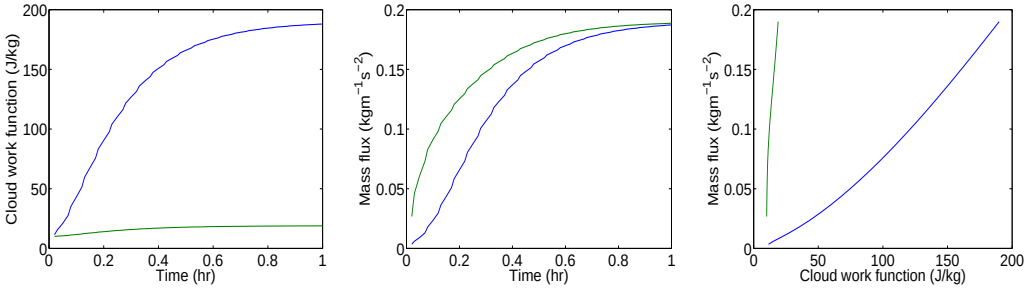

Figure 8: Example solution for the unforced $p = 2$ system with parameters chosen to illustrate region II of Fig. 6. Blue is for the deep mode and green for the shallow mode. The parameters are $\tau_d = \tau_s = 10^2$ s, together with the default choices for α, β and γ described in Section 3.2. These choices give $\hat{\gamma}_s = 10^{-3}$ s^{-1} and $\hat{\gamma}_d = 2 \times 10^{-3}$ s^{-1}, so that $\hat{\gamma}_s + 1/8\tau_s > \hat{\gamma}_d > \hat{\gamma}_s$. Shown in the same format as in Fig. 2.

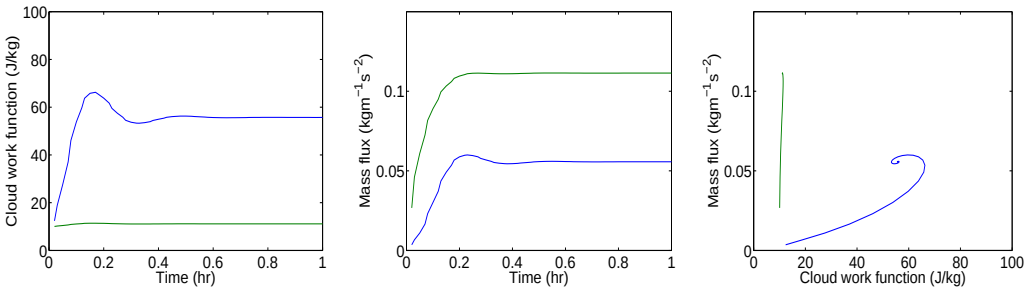

Figure 9: Example solution for the unforced $p = 2$ system with parameters chosen to illustrate region III of Fig. 6. Blue is for the deep mode and green for the shallow mode. The parameters are $\gamma_d = 8, \gamma_s = 0.1, \beta_d = 0.2, \beta_s = 4$ Jm^2 kg^{-2} and $\tau_d = \tau_s = 10^2$ s, together with the default choices for α_s and α_d described in Section 3.2. These choices give $\hat{\gamma}_s = 10^{-3}$ s^{-1} and $\hat{\gamma}_d = 8 \times 10^{-3}$ s^{-1}, so that $\hat{\gamma}_d > \hat{\gamma}_s + 1/8\tau_s$. Shown in the same format as in Fig. 2.

4.6.2. With a slight deviation from $\tau_s = \tau_d$

We now consider unequal τ but with the shallow and deep time scales being close together. The question is whether a distinction between the time scales is able to alter the phase diagram in such a way as to be able to produce a periodic solution.

We introduce the notation

$$\Delta\xi \equiv (\xi_s - \xi_d)/2 \tag{4.6.7}$$

with

$$\begin{aligned} \xi_d &= \xi - \Delta\xi \\ \xi_s &= \xi + \Delta\xi \quad . \end{aligned} \tag{4.6.8}$$

We furthermore introduce

$$\tau_0 \equiv (\tau_s + \tau_d)/2$$
$$\Delta\tau \equiv \tau_s - \tau_d \tag{4.6.9}$$

so that the relation

$$\Delta\xi = \sigma^2(\tau_s - \tau_d) = \sigma^2\Delta\tau. \tag{4.6.10}$$

follows immediately from the definition of terms. The assumption that the two time scales are close together means that we can take $\xi \gg |\Delta\xi|$ or $\tau \gg |\Delta\tau|$ below.

The eigenfrequency equation for any values of τ was stated as Eq. 4.6.2 above. In the limit of equal shallow and deep time scales it reduces to Eq. 4.6.3 giving us the zeroth–order solution $\xi \equiv \xi_0 = 0$ or $\hat{\gamma}_s - \hat{\gamma}_d$ just as in Eq. 4.6.4, with corresponding eigenfrequencies as given in Eq. 4.6.5. With the subscript zero denoting a zeroth–order quantity, these are

$$\sigma_0 = -\frac{1}{4\tau_0} \pm \left[\left(\frac{1}{4\tau_0}\right)^2 + \frac{\xi_0}{2\tau_0}\right]^{1/2}. \tag{4.6.11}$$

To obtain the leading corrections to these results for a difference in time scales, we write $\xi = \xi_0 + \xi_1$ and expand the eigenfrequency equation 4.6.2 to include first order terms in $\Delta\xi$ and ξ_1. We first note that

$$\xi_s\xi_d = (\xi_0 + \xi_1 + \Delta\xi)(\xi_0 + \xi_1 - \Delta\xi) = (\xi_0 + \xi_1)^2 - \Delta\xi^2 \simeq \xi_0^2 + 2\xi_1\xi_0 \tag{4.6.12}$$

so that $\Delta\xi$ does not enter into this expression. As a result, at first order Eq. 4.6.2 is

$$2\xi_0\xi_1 + (\hat{\gamma}_d + \hat{\gamma}_s)\Delta\xi + (\hat{\gamma}_d - \hat{\gamma}_s)\xi_1 = 0 \tag{4.6.13}$$

or

$$(2\xi_0 + \hat{\gamma}_d - \hat{\gamma}_s)\xi_1 + (\hat{\gamma}_d + \hat{\gamma}_s)\Delta\xi = 0 \tag{4.6.14}$$

leading to

$$\xi_1 = -(2\xi_0 + \hat{\gamma}_d - \hat{\gamma}_s)^{-1}(\hat{\gamma}_d + \hat{\gamma}_s)\Delta\xi. \tag{4.6.15}$$

For the case of $\xi_0 = 0$ we have $\sigma_0 = 0$ or $\sigma_0 = -1/(2\tau_0)$. The first of these possibilities gives $\Delta\xi = 0$ at leading order and so $\xi_1 = 0$. The second possibility gives

$$\xi_1 = -\left(\frac{\hat{\gamma}_d + \hat{\gamma}_s}{\hat{\gamma}_d - \hat{\gamma}_s}\right)\frac{\tau_s - \tau_d}{4\tau_0^2} = -\lambda_1\Delta\xi \tag{4.6.16}$$

where we have defined

$$\lambda_1 \equiv \frac{\hat{\gamma}_d + \hat{\gamma}_s}{\hat{\gamma}_d - \hat{\gamma}_s} \tag{4.6.17}$$

For the case of $\xi_0 = \hat{\gamma}_s - \hat{\gamma}_d$ we have

$$\xi_1 = \lambda_1\Delta\xi. \tag{4.6.18}$$

Eqs. 4.6.16 and 4.6.18 are the first order corrections to each of the solutions to ξ. However, we wish to translate these corrections into the corresponding corrections to the eigenfrequencies σ. In order to make this translation we write $\sigma = \sigma_0 + \sigma_1$, substitute this form into the definition for either of ξ_s or ξ_d (Eq. 4.6.1) and expand all variables to first order in the time scale difference. The result is that

$$\sigma_1 = \frac{\xi_1}{4\sigma_0\tau_0 + 1}. \tag{4.6.19}$$

So for the non-trivial case with $\xi_0 = 0$ we have

$$\sigma_0 = -\frac{1}{2\tau_0} \qquad \sigma_1 = -\xi_1 = \lambda_1\Delta\xi \tag{4.6.20}$$

so that

$$\sigma = -\frac{1}{2\tau_0} + \left(\frac{\hat{\gamma}_d + \hat{\gamma}_s}{\hat{\gamma}_d - \hat{\gamma}_s}\right)\frac{\tau_s - \tau_d}{4\tau_0^2} + \mathcal{O}(\tau_s - \tau_d)^2 \tag{4.6.21}$$

which is a real correction to a real eigenvalue.

For the case of $\xi_0 = \hat{\gamma}_s - \hat{\gamma}_d$ we have

$$\sigma_0 = -\frac{1}{4\tau_0} \pm \lambda_0 \qquad \sigma_1 = \pm\frac{\lambda_1}{\lambda_0}\frac{\Delta\xi}{4\tau_0} = \pm\frac{\lambda_1}{\lambda_0}\sigma_0^2\frac{\Delta\tau}{4\tau_0} \tag{4.6.22}$$

where

$$\lambda_0 = \frac{1}{4\tau_0}\left[1 + 8\tau_0(\hat{\gamma}_s - \hat{\gamma}_d)\right]^{1/2}. \tag{4.6.23}$$

By further using the relation

$$\sigma_0^2 = \frac{1}{(4\tau_0)^2} + \lambda_0^2 \mp \frac{\lambda_0}{2\tau_0} \tag{4.6.24}$$

we obtain the following expression for the correction term

$$\sigma_1 = \pm\frac{\lambda_1}{\lambda_0}\frac{(\tau_s - \tau_d)}{4\tau_0}\left[\frac{1}{(4\tau_0)^2} + \lambda_0^2 \mp \frac{\lambda_0}{2\tau_0}\right]. \tag{4.6.25}$$

In total we obtain

$$\sigma = -\frac{1}{4\tau_0} \pm \lambda_0\left\{1 + \lambda_1\frac{(\tau_s - \tau_d)}{4\tau_0}\left[1 + \frac{1}{(4\tau_0\lambda_0)^2} \mp \frac{1}{2\tau_0\lambda_0}\right]\right\}. \tag{4.6.26}$$

Since λ_1 is real, the eigenvalue as a whole must be real unless λ_0 is imaginary. Simple inspection of Eq. 4.6.23 shows that this requires $\hat{\gamma}_d > \hat{\gamma}_s + (1/8\tau_0)$ as was already derived for the case of equal time scales in the previous subsection. Assuming that λ_0 is indeed imaginary, the next question to ask is whether there are circumstances in which the real part of the eigenvalue vanishes. If so then a periodic solution can indeed be obtained.

The real part of the eigenvalue in this case is

$$-\frac{1}{4\tau_0} - \lambda_0\left\{\lambda_1\frac{(\tau_s - \tau_d)}{4\tau_0}\frac{1}{2\tau_0\lambda_0}\right\} = -\frac{1}{4\tau_0}\left[1 + \lambda_1(\tau_s - \tau_d)\frac{1}{2\tau_0}\right] \tag{4.6.27}$$

which will vanish if

$$\tau_d - \tau_s = \frac{2\tau_0}{\lambda_1} = 2\tau_0 \left(\frac{\hat{\gamma}_d + \hat{\gamma}_s}{\hat{\gamma}_d - \hat{\gamma}_s} \right). \tag{4.6.28}$$

Given that $\hat{\gamma}_d$ and $\hat{\gamma}_s$ are positive, the factor in brackets in the above equation can have a modulus that is no smaller than unity. Thus, in order for the real part to vanish the difference between the shallow and deep time scales must be larger than twice the mean time scale. Since this contradicts our original assumption that the time scale difference can be treated as a perturbation, the conclusion must be that a periodic solution cannot be obtained for a small time scale difference.

We have checked this analysis numerically by solving the full eigenvalue equation for cases where τ_s is 10% larger than τ_d and vice versa. The resulting phase diagrams are shown in Fig. 10 and may be compared with Fig. 6. The lines separating regions I/II and II/III have different slopes for $\tau_s \neq \tau_d$ and so tend towards each other in a part of phase space. In summary then, the analysis of this subsection does raise the possibility that the system can produce a periodic solution, but demonstrates that this will not occur in practice unless there is a substantial difference between the shallow and deep time scales.

4.6.3. When $\tau_s \ll \tau_d$

Having established that a periodic solution does not occur for $\tau_s = \tau_d$ (Section 4.6.1) or for $\tau_s \approx \tau_d$ (Section 4.6.2), the natural next step in the analysis is to consider the behaviour of the system when these two time scales are well separated. In the present subsection we consider $\tau_s \ll \tau_d$, and in the following subsection we will consider $\tau_s \gg \tau_d$.

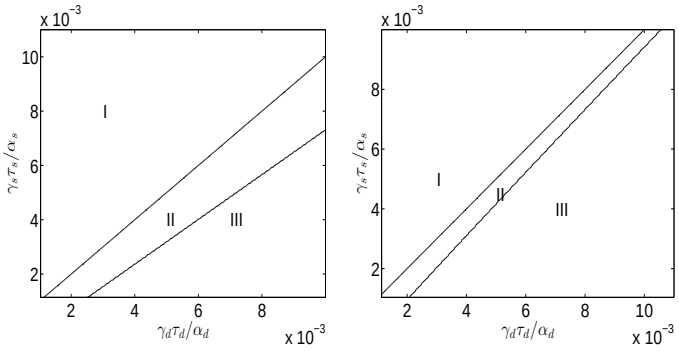

Figure 10: As in Fig. 6 but plotted for $\tau_s = 110$ s (left) and for $\tau_d = 110$ s (right), all other parameters remaining unchanged.

Starting from the eigenvalue equation as expressed by Eqs. 4.6.1 and 4.6.2, the limit of $\tau_s \ll \tau_d$ can be considered by setting $\xi_s \simeq \sigma$ while retaining the full formula defining ξ_d. As a result, Eq. 4.6.2 reduces to

$$\sigma^2(2\sigma\tau_d + 1) + \hat{\gamma}_d\sigma - \hat{\gamma}_s\sigma(2\sigma\tau_d + 1) \simeq 0 \tag{4.6.29}$$

or

$$\sigma^2 + \frac{1}{2\tau_d}(1 - 2\tau_d\hat{\gamma}_s)\sigma + \frac{1}{2\tau_d}(\hat{\gamma}_d - \hat{\gamma}_s) \simeq 0 \tag{4.6.30}$$

which has the solution

$$4\tau_d\sigma \simeq -(1 - 2\tau_d\hat{\gamma}_s) \pm [(1 + \tau_d\hat{\gamma}_s)^2 - 8\tau_d\hat{\gamma}_d]^{1/2}. \tag{4.6.31}$$

The solution is oscillatory when $8\tau_d\hat{\gamma}_d > (1 + \tau_d\hat{\gamma}_s)^2$, and it becomes purely oscillatory when $\tau_d\hat{\gamma}_s = 1/2$. Substituting the latter condition into the former we find that the conditions for a pure oscillation can be written as

$$\tau_d\hat{\gamma}_s = 1/2 \quad \text{and} \quad \hat{\gamma}_d < (9/16)\hat{\gamma}_s. \tag{4.6.32}$$

Hence, the self–amplification rate, $\hat{\gamma}_s$, of shallow convection must balance with the self–dissipation rate, τ_d^{-1}, of deep convection in order to obtain a purely oscillatory solution. Moreover, the self–dampening of deep convection through $\hat{\gamma}_d$ should not be too strong.

4.6.4. When $\tau_s \gg \tau_d$

Now we briefly consider the opposite limit of $\tau_s \gg \tau_d$, repeating a similar procedure as in Section 4.6.3. The eigenvalue equation in this limit is

$$\sigma^2 + \frac{1}{2\tau_s}(1 + 2\tau_s\hat{\gamma}_d)\sigma + \frac{1}{2\tau_s}(\hat{\gamma}_d - \hat{\gamma}_s) \simeq 0 \tag{4.6.33}$$

which has the solution

$$4\tau_s\sigma \simeq -(1 + 2\tau_s\hat{\gamma}_d) \pm [(1 - \tau_s\hat{\gamma}_d)^2 + 8\tau_s\hat{\gamma}_s]^{1/2} \tag{4.6.34}$$

In this limit the eigenvalues are real for any choice of parameters.

4.7. The $p = 2$ equations with vanishing determinant: Periodic solution

In Section 4.6 we considered various special or approximate cases of the unforced coupled $p = 2$ system. A periodic solution can arise in which the growing and dampening tendencies of the system are offset against each other. This can only be achieved for a careful choice of the parameters and, in particular, it does not occur for our default set described in Section 3.2 since that has $\tau_s = \tau_d$. Here we consider what constraints on the parameters must be satisfied for a periodic solution. Unlike the previous subsection, we do not seek to understand the behaviour of the system in any limiting regime, but rather consider the general constraints.

Assuming a periodic solution, we can write $\sigma = i\omega$ where ω is real. Substituting this form into the eigenvalue equation 4.5.7, and examining its real and imaginary parts produces

$$\frac{-\omega^2}{2}\left(\frac{1}{\tau_d}+\frac{1}{\tau_s}\right)+\frac{1}{4\tau_d\tau_s}(\hat{\gamma}_d-\hat{\gamma}_s)=0$$

or

$$\omega^2=\frac{\hat{\gamma}_d-\hat{\gamma}_s}{2(\tau_d+\tau_s)} \tag{4.7.1}$$

for the real part, and

$$-\omega^3+\frac{\omega}{4}\left[\frac{1}{\tau_d\tau_s}+2\left(\frac{\hat{\gamma}_d}{\tau_d}-\frac{\hat{\gamma}_s}{\tau_s}\right)\right]=0$$

or

$$\omega^2=\frac{1}{4}\left[\frac{1}{\tau_d\tau_s}+2\left(\frac{\hat{\gamma}_d}{\tau_d}-\frac{\hat{\gamma}_s}{\tau_s}\right)\right] \tag{4.7.2}$$

for the imaginary part. Both equations for ω must be satisfied simultaneously to realize a periodic solution, which produces the following constraint on the parameters.

$$\frac{\hat{\gamma}_d-\hat{\gamma}_s}{2(\tau_d+\tau_s)}=\frac{1}{4}\left[\frac{1}{\tau_d\tau_s}+2\left(\frac{\hat{\gamma}_d}{\tau_d}-\frac{\hat{\gamma}_s}{\tau_s}\right)\right] \tag{4.7.3}$$

This can be rearranged to read

$$\tau_d^2\hat{\gamma}_s-\tau_s^2\hat{\gamma}_d=\frac{\tau_d+\tau_s}{2} \tag{4.7.4}$$

This is a necessary but not sufficient condition since it must be checked that the resulting ω is indeed real. From Eq. 4.7.1 this requires that $\hat{\gamma}_d > \hat{\gamma}_s$. An interesting consequence of these conditions can immediately be recognized. Rewriting Eq. 4.7.4 as

$$\hat{\gamma}_d=\left(\frac{\tau_d}{\tau_s}\right)^2\hat{\gamma}_s-\left(\frac{\tau_d+\tau_s}{2\tau_s^2}\right) \tag{4.7.5}$$

it follows that a periodic solution requires $\tau_d > \tau_s$.

It is straightforward to check that the general constraints of Eq. 4.7.4 and $\hat{\gamma}_d > \hat{\gamma}_s$ are consistent with the constraints previously derived for particular special cases and limits.

- For the case of $\tau_s = \tau_d = \tau$ as considered in Section 4.6.1, Eq. 4.7.4 gives $\hat{\gamma}_s - \hat{\gamma}_d = \tau^{-1}$ which violates the constraint $\hat{\gamma}_d > \hat{\gamma}_s$ and so there is no periodic solution.

- In the limit of $\tau_s \ll \tau_d$ as considered in Section 4.6.3, Eq. 4.7.4 immediately gives $\tau_d \hat{\gamma}_s = 1/2$ as derived previously.

- In the limit of $\tau_d \ll \tau_s$ as considered in Section 4.6.4, Eq. 4.7.4 immediately gives $\tau_s \hat{\gamma}_d = -1/2$ which cannot be satisfied and so there is no periodic solution.

4.8. Summary of results for the coupled $p = 2$ system

The system of Eqs. 4.0.8 and 4.0.9 arises from Arakawa and Schubert's (1974) energy cycle description for a system with two types of convection, along with Pan and Randall's (1998) assumption for the relationship between convective kinetic energy and cloud–base mass flux. All of the parameters in those equations are assumed to be positive in accordance with the arguments presented in Section 2.

The main results arising from our analysis of the system are that:

- The unforced shallow system is unstable in isolation (Section 4.1) whereas the unforced deep system in isolation has vanishing convective activity (Section 4.2).

- The coupled system may be unstable, damping or neutral according to the parameter settings. It may also exhibit periodicity. These possibilities were simply demonstrated for a limiting case where the mass fluxes equilibriate much more quickly than the cloud work function (Section 4.3).

- Solutions of particular interest are those for which the destabilizing and stabilizing tendencies of shallow and deep convection respectively are balanced. A necessary condition for such a solution is that the determinant of the interaction matrix $\mathcal{K}$ should vanish (Section 4.4.1; Eq. 4.4.2).

- Assuming a vanishing determinant:

  - The solution takes the form of Eq. 4.5.4, with formulae for the coefficients being given in Section 4.5 and the cubic eigenfrequency equation being given in Eq. 4.5.7.

  - A necessary condition to avoid an exploding solution is that $\hat{\gamma}_d \geq \hat{\gamma}_s$ (Section 4.5; Eq. 4.5.9). If the solution does not explode, it will either decay towards an equilibrium configuration (possibly an oscillatory decay), or else it may produce persistent oscillations.

  - Persistent oscillations require the parameters to satisfy a further constraint, Eq. 4.7.4. They will not occur for $\tau_s = \tau_d$ (Section 4.6.1) or for $\tau_s \approx \tau_d$ (Section 4.6.2), but can only occur if $\tau_d > \tau_s$ (Sections 4.6.3, 4.6.4 and 4.7).

5. Analysis of the system: the $p = 1$ case

In Section 4 we have investigated the energy-cycle system arising from the use of $p = 2$ in Eq. 3.1.3. As discussed in Section 3.1, an alternative choice of $p = 1$ is also an attractive possibility with a distinct physical interpretation. Setting $p = 1$ in Eq. 3.1.3 and substituting into Eqs. 3.1.1 and 3.1.2, the energy-cycle equations read

$$\begin{aligned} \dot{M}_d &= \frac{M_d}{\tau_d}\left(\frac{A_d - A_{d0}}{A_{d0}}\right) \\ \dot{M}_s &= \frac{M_s}{\tau_s}\left(\frac{A_s - A_{s0}}{A_{s0}}\right) \end{aligned} \tag{5.0.1}$$

$$\begin{aligned} \dot{A}_d &= \beta_s M_s - \gamma_d M_d + F_d \\ \dot{A}_s &= \gamma_s M_s - \beta_d M_d + F_s \end{aligned} \tag{5.0.2}$$

where

$$\begin{aligned} A_{d0} &= \frac{\alpha_d}{\tau_d} \\ A_{s0} &= \frac{\alpha_s}{\tau_s}. \end{aligned} \tag{5.0.3}$$

The analysis of the nonlinear $p = 1$ case in this section proceeds along similar lines as for the linear $p = 2$ case in the previous section. Thus, we begin by considering shallow and deep convection separately in Sections 5.1 and 5.2 respectively. The coupled system is considered in general terms in Sections 5.3 to 5.5 and its behaviour is exemplified by some useful linearizations presented in Sections 5.6 and 5.7. A summary of the results obtained is provided in Section 5.8.

Since the $p = 1$ system is nonlinear, it is convenient to describe it in terms of nondimensional parameters from the outset, as seen below. We introduce

nondimensional couplings by

$$\hat{\gamma}_d = \frac{\gamma_d \tau_s \tau_d M_{d0}}{\alpha_d} = \frac{\gamma_d \tau_s M_{d0}}{A_{d0}}, \qquad \hat{\beta}_d = \frac{\beta_d \tau_s^2 M_{d0}}{\alpha_s} = \frac{\beta_d \tau_s M_{d0}}{A_{s0}}$$
$$\hat{\gamma}_s = \frac{\gamma_s \tau_s^2 M_{s0}}{\alpha_s} = \frac{\gamma_s \tau_s M_{s0}}{A_{s0}}, \qquad \hat{\beta}_s = \frac{\beta_s \tau_s \tau_d M_{s0}}{\alpha_d} = \frac{\beta_s \tau_s M_{s0}}{A_{d0}} \quad (5.0.4)$$

The reader should note that these rescaled coupling parameters are defined differently from Eq. 4.3.4 which introduced notation convenient for analysis of the $p = 2$ system. Since the $p = 2$ and $p = 1$ systems are analysed in separate sections of this article there can be no scope for confusion. Here we have introduced arbitrary constants M_{d0} and M_{s0} to describe typical values of the mass fluxes for deep and shallow convection respectively. Rather than choosing values for these parameters, it is convenient to choose instead particular values for the nondimensional parameters $\hat{\gamma}_s$ and $\hat{\gamma}_d$ and then to use the definition of those parameters in order to set M_{s0} and M_{d0}. Specifically we take

$$\hat{\gamma}_s = 1, \qquad \hat{\gamma}_d = 1 \quad (5.0.5)$$

so that

$$M_{d0} = \frac{\alpha_d}{\gamma_d \tau_s \tau_d}$$
$$M_{s0} = \frac{\alpha_s}{\gamma_s \tau_s^2} \quad (5.0.6)$$

and

$$\hat{\beta}_d = \frac{\alpha_d \beta_d \tau_s}{\alpha_s \gamma_d \tau_d}$$
$$\hat{\beta}_s = \frac{\alpha_s \beta_s \tau_d}{\alpha_d \gamma_s \tau_s}. \quad (5.0.7)$$

It is also convenient to define a parameter for the ratio of shallow and deep time scales,

$$\mu = \frac{\tau_s}{\tau_d}. \tag{5.0.8}$$

Using the default parameter set discussed in Section 3.2 the parameters introduced in the present section take the values $M_{s0} = 10^{-2}$ kgm^{-2}s^{-1}, $M_{d0} = 5 \times 10^{-3}$ kgm^{-2}s^{-1}, $\hat{\beta}_s = 2$, $\hat{\beta}_d = 1/2$ and $\mu = 1$. These mass flux scalings are consistent with typical values, as estimated for example by Yano and Plant (2012b).

5.1. Shallow convection only

The equations for the shallow mode only are (with dimensional variables)

$$\begin{aligned} \dot{M}_s = &\quad \frac{M_s}{\tau_s}\left(\frac{A_s - A_{s0}}{A_{s0}}\right) \\ \dot{A}_s = &\quad F_s + \gamma_s M_s. \end{aligned} \tag{5.1.1}$$

As before, we neglect any large-scale forcing of shallow convection so that $F_s = 0$. We also non-dimensionalize this system in terms of the scaling parameter for shallow mass flux, M_{s0}, that was introduced above, and the stationary value, A_{s0} for the shallow cloud work function. Specifically,

$$M_s = M_{s0} x_s, \qquad A_s = A_{s0}(1 + y_s) \tag{5.1.2}$$

so that x_s and y_s are the nondimensionalized mass flux and cloud work function respectively. We furthermore nondimensionalize time with τ_s to obtain

$$\begin{aligned} \dot{x}_s = &\quad x_s y_s \\ \dot{y}_s = &\quad \hat{\gamma}_s x_s \end{aligned} \tag{5.1.3}$$

using the nondimensional parameter $\hat{\gamma}_s$ defined above. These equations are further simplified by recalling that, without loss of generality, we set $\hat{\gamma}_s = 1$ above.

The shallow-only equations may be rewritten as

$$\frac{dx_s}{x_s y_s} = \frac{dy_s}{x_s} = dt \tag{5.1.4}$$

from which the first equality gives

$$dx_s = y_s dy_s. \tag{5.1.5}$$

This can be readily integrated to obtain the path of the system in phase space:

$$x_s = \frac{1}{2}(y_s^2 - y_s(0)^2) + x_s(0). \tag{5.1.6}$$

Substitution into the cloud work function equation leads to

$$\dot{y}_s = \frac{1}{2}(y_s^2 - y_s(0)^2) + x_s(0) \equiv \frac{1}{2}(y_s^2 - r_s^2). \tag{5.1.7}$$

Thus, the behaviour of the solution depends on the combination $r_s^2 \equiv y_s(0)^2 - 2x_s(0)$ from the initial conditions. For $r_s^2 < 0$ the cloud work function must increase without limit, and likewise the mass flux will explode, as can be readily seen from its tendency equation. For $r_s^2 = 0$, we have

$$\dot{y}_s = \frac{1}{2}y_s^2 \tag{5.1.8}$$

which is easily integrated to give

$$y_s = \frac{2}{2/y_s(0) - t}. \tag{5.1.9}$$

In this case the cloud work function (and the mass flux) explodes to infinity at $t = 2/y_s(0)$ (recall that the nondimensional t is defined in units of τ_s) if

its initial value is larger than the equilibrium value (*i.e.*, $y_s(0) > 0$) or else it approaches the equilibrium value (with vanishing mass flux) if the initial value is smaller than this. For $r_s^2 > 0$, the solution for the cloud work function is

$$y_s = -r_s \left[\left(\frac{y_s(0) - r_s}{y_s(0) + r_s} \right) e^{r_s t} + 1 \right] \left[\left(\frac{y_s(0) - r_s}{y_s(0) + r_s} \right) e^{r_s t} - 1 \right]^{-1} . \qquad (5.1.10)$$

In this case, the cloud work function tends to a stationary value of $-r_s$ as $t \to \infty$. In the final state, the mass flux vanishes. Examples of exploding and decaying solutions of the unforced shallow equations are shown in Figs. 11 and 12 respectively.

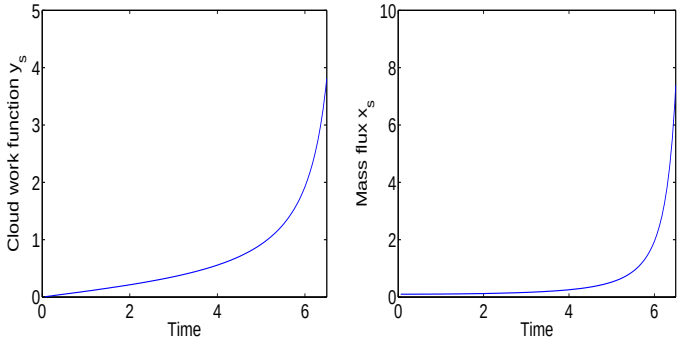

Figure 11: Example solution of an exploding case for the unforced shallow mode alone in the $p = 1$ system. The parameters are the default set described in Section 3.2, giving scaling factors of $A_{s0} = 1$ Jkg^{-1}, $M_{s0} = 10^{-2}$ kgm^{-2}s^{-1} and $\tau_s = 10^3$ s. The initial conditions are $x_s(0) = 0.1$, $y_s(0) = 0$ so that $r_s^2 = -0.2$. On the left and right respectively are shown the time series of the nondimensionalized cloud work function and of the nondimensionalized mass flux.

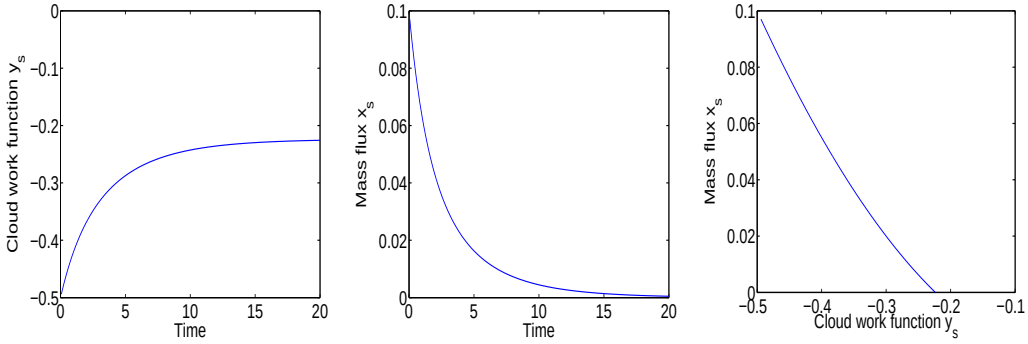

Figure 12: Example solution of a decaying case for the unforced shallow mode alone in the $p = 1$ system. The parameters are the default set described in Section 3.2, giving scaling factors of $A_{s0} = 1$ Jkg^{-1}, $M_{s0} = 10^{-2}$ kgm^{-2}s^{-1} and $\tau_s = 10^3$ s. The initial conditions are $x_s(0) = 0.1$, $y_s(0) = -0.5$ so that $r_s^2 = 0.05$. From left to right are shown: the time series of the nondimensionalized cloud work function, the time series of the nondimensionalized mass flux, and the trajectory in the phase space of the nondimensionalized cloud work function (horizontal axis) and the nondimensionalized mass flux (vertical axis).

5.2. Deep convection only

The equations for the deep mode only are (with dimensional variables)

$$\begin{aligned} \dot{M}_d = &\quad \frac{M_d}{\tau_d}\left(\frac{A_d - A_{d0}}{A_{d0}}\right) \\ \dot{A}_d = &\quad F_d - \gamma_d M_d \end{aligned} \tag{5.2.1}$$

As before, we neglect any large-scale forcing of deep convection, $F_d = 0$. We also non-dimensionalize this system in terms of the scaling parameter for deep mass flux, M_{d0}, and the stationary value, A_{d0} for the deep cloud work function. Specifically,

$$M_d = M_{d0} x_d, \qquad A_d = A_{d0}(1 + y_d) \tag{5.2.2}$$

so that x_d and y_d are the nondimensionalized mass flux and cloud work function respectively. Anticipating later analysis of the coupled system we furthermore nondimensionalize the time by using τ_s rather than τ_d, to obtain

$$\begin{aligned} \dot{x}_d &= \mu x_d y_d \\ \dot{y}_d &= -\hat{\gamma}_d x_d \end{aligned} \tag{5.2.3}$$

using the nondimensional parameters defined above. These equations are further simplified by recalling that, without loss of generality, we set $\hat{\gamma}_d = 1$ above.

The deep-only equations may rewritten as

$$\frac{dx_d}{\mu x_d y_d} = -\frac{dy_d}{x_d} = dt \tag{5.2.4}$$

As for the isolated shallow–convection system, the first equality can be readily integrated to give a phase–space solution,

$$x_d = -\frac{\mu}{2}(y_d^2 - y_d(0)^2) + x_d(0). \tag{5.2.5}$$

Substitution of the orbit equation into the cloud work function equation leads to

$$\dot{y}_d = -\frac{\mu}{2}(y_d^2 - y_d(0)^2) + x_d(0) \equiv -\frac{\mu}{2}(y_d^2 - r_d^2). \tag{5.2.6}$$

Thus, the behaviour of the solution depends on the combination $r_d^2 \equiv y_d(0)^2 + (2/\mu)x_d(0)$ from the initial conditions. This combination is guaranteed to be positive and the resulting cloud work function evolution is given by

$$y_d = -r_d \left[1 + \left(\frac{y_d(0) - r_d}{y_d(0) + r_d}\right) e^{-\mu r_d t}\right] \left[1 - \left(\frac{y_d(0) - r_d}{y_d(0) + r_d}\right) e^{-\mu r_d t}\right]^{-1}. \tag{5.2.7}$$

The cloud work function approaches $-r_d$ (and the mass flux vanishes) as $t \to \infty$. Examples solutions of the unforced deep equations are shown in

Figs. 13 and 14 for cases of initial growth ($y_d(0) > 0$) or decay ($y_d(0) < 0$) respectively.

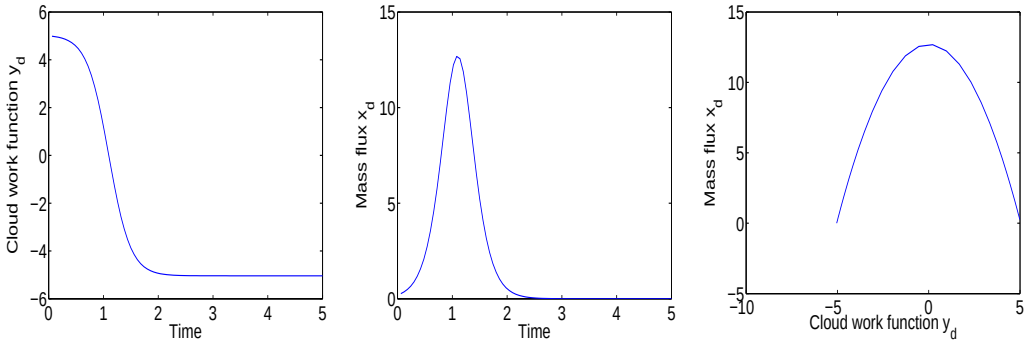

Figure 13: Example solution for the unforced deep mode alone in the $p = 1$ system: a case with a single episode. The parameters are the default set described in Section 3.2, giving scaling factors of $A_{d0} = 10$ Jkg^{-1}, $M_{d0} = 5 \times 10^{-3}$ kgm^{-2}s^{-1} and $\tau_s = 10^3$ s. The initial conditions are $x_d(0) = 0.2$, $y_d(0) = 5$. Shown in the same format as in Fig. 12.

5.3. General case

We now proceed to discuss the coupled $p = 1$ system. The relevant dimensional equations are given in Eqs. 5.0.1 and 5.0.2, and the forcings will again be set to zero. In terms of the dimensionless parameters and variables introduced by Eqs. 5.0.4–5.0.8, 5.1.2 and 5.2.2 these equations read

$$\dot{x}_s = x_s y_s \tag{5.3.1a}$$

$$\dot{x}_d = \mu x_d y_d \tag{5.3.1b}$$

$$\dot{y}_s = x_s - \hat{\beta}_d x_d \tag{5.3.1c}$$

$$\dot{y}_d = -x_d + \hat{\beta}_s x_s. \tag{5.3.1d}$$

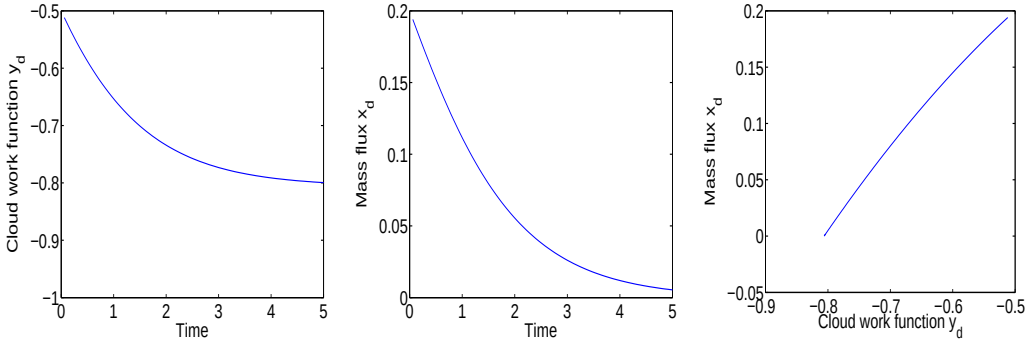

Figure 14: example solution for the unforced deep mode alone in the $p = 1$ system: a case with simple decay. The parameters are the default set described in Section 3.2, giving scaling factors of $A_{d0} = 10$ Jkg^{-1}, $M_{d0} = 5 \times 10^{-3}$ kgm^{-2}s^{-1} and $\tau_s = 10^3$ s. The initial conditions are $x_d(0) = 0.2$, $y_d(0) = -0.5$. Shown in the same format as in Fig. 12.

As with the coupled $p = 2$ system, our main interest is whether the possible explosive growth of shallow convection and the damping of deep convection can be coupled in such a way as to produce self–perpetuating behaviour, with deep convection acting as a break on shallow convection and shallow convection in turn providing a surrogate forcing for deep convection. Recalling Section 4.4.1, we note that a vanishing determinant for the $\mathcal{K}$ matrix is a necessary condition for such behaviour, irrespective of the choice of p. The corresponding constraint on the parameters is as stated in Eq. 4.4.2, and in non-dimensional units, this takes the form

$$\hat{\beta}_s \hat{\beta}_d = 1. \tag{5.3.2}$$

Asssuming a vanishing determinant, the cloud work functions for shallow and deep convection are linked together by Eq. 4.4.6, or in nondimensional

units

$$y_s - y_s(0) = \hat{\beta}_d \left(y_d - y_d(0) \right). \tag{5.3.3}$$

5.4. The $p = 1$ equations with vanishing determinant: General considerations

Using Eq. 5.3.3 (relating the cloud work functions) in Eq. 5.3.1a (the evolution equation for shallow mass flux) we find

$$\dot{x}_s = x_s y_s(0) + \hat{\beta}_d x_s \left(y_d - y_d(0) \right). \tag{5.4.1}$$

The deep cloud work function y_d can then be eliminated by substituting from Eq. 5.3.1b to produce

$$\frac{\dot{x}_s}{x_s} = \frac{\hat{\beta}_d}{\mu} \frac{\dot{x}_d}{x_d} + y_s(0) - \hat{\beta}_d y_d(0). \tag{5.4.2}$$

Thus, in order to obtain a closed solution in phase space, an additional constraint on the initial conditions is required. Specifically, the initial cloud work functions must be related by

$$y_s(0) = \hat{\beta}_d y_d(0) \tag{5.4.3}$$

because otherwise the integration of Eq. 5.4.2 will produce a term proportional to time. We call this condition the *initial periodicity condition*. A consequence is that the two nondimensionalized cloud work functions are then proportional for all times, as can be seen from Eq. 5.3.3. Clearly the condition is satisfied if both cloud work functions start from their equilibrium values, $y_s(0) = y_d(0) = 0$.

A vanishing determinant and initial periodicity are necessary conditions for the periodicity of a solution to the coupled system, but they are not sufficient conditions. We investigate the coupled system further below assuming

the initial periodicity to hold. For the remainder of this subsection, however, we examine the character of the solutions when the initial periodicity condition is not met. In order to do so, it is convenient to introduce some further notation, defining the dimensionless parameters

$$q = \frac{\hat{\beta}_d}{\mu} = \frac{\beta_d \alpha_d}{\gamma_d \alpha_s} \tag{5.4.4}$$

and

$$r_c = y_s(0) - \hat{\beta}_d y_d(0). \tag{5.4.5}$$

The initial periodicity condition corresponds to $r_c = 0$, while for the default parameters described in Section 3.2 we have $q = 1/2$. In terms of these parameters, Eq. 5.4.2 can be expressed as

$$\frac{\dot{x}_s}{x_s} = q\frac{\dot{x}_d}{x_d} + r_c. \tag{5.4.6}$$

Integration of the above equation gives

$$\frac{x_s}{x_s(0)} = \left(\frac{x_d}{x_d(0)}\right)^q e^{r_c t}. \tag{5.4.7}$$

For $r_c > 0$ then $x_s \gg x_d$ as $t \to \infty$ so that deep convection becomes negligible and the system approaches the behaviour of the one-mode shallow-only system. As discussed in Section 5.1, that system may either explode or decay to zero activity. Likewise, for $r_c < 0$ then $x_s \ll x_d$ as $t \to \infty$ so that shallow convection becomes negligible and the system approaches the behaviour of the one-mode deep-only system. As discussed in Section 5.2 that system will always decay to zero activity. Examples of numerical solutions to the coupled equations for $r_c > 0$ and $r_c < 0$ are shown in Figs. 15 and 16 respectively.

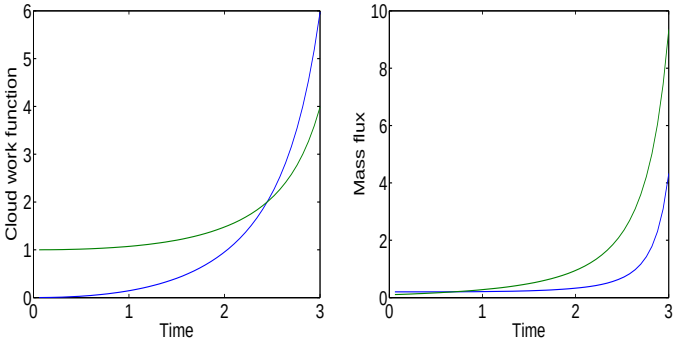

Figure 15: Example solution for the unforced $p = 1$ system with parameters chosen to violate the initial periodicity condition, and with $r_c > 0$. Blue is for the deep mode and green for the shallow mode. The parameters are the default set described in Section 3.2, giving scaling factors of $A_{d0} = 10$ Jkg^{-1}, $A_{s0} = 1$ Jkg^{-1}, $M_{d0} = 5 \times 10^{-3}$ kgm^{-2}s^{-1}, $M_{s0} = 10^{-2}$ kgm^{-2}s^{-1} and $\tau_s = \tau_d = 10^3$ s. The initial conditions are $x_d(0) = 0.2$, $x_s(0) = 0.1$, $y_d(0) = 0$ and $y_s(0) = 1$ so that $r_c = 1$. Shown in the same format as in Fig. 11.

5.5. Behaviour of the system with initial periodicity condition

We now consider the character of the solution assuming both a vanishing determinant and the initial periodicity condition, $r_c = 0$. The key issue is to identify whether any additional conditions are required in order to obtain a periodic solution.

When initial periodicity holds, the relationship between shallow and deep mass flux in Eq. 5.4.7 reduces to

$$\frac{x_s}{x_s(0)} = \left(\frac{x_d}{x_d(0)} \right)^q \tag{5.5.1}$$

The path of the solution in phase space can also be derived for the other variables. For example, a solution in terms of the deep variables x_d, y_d can

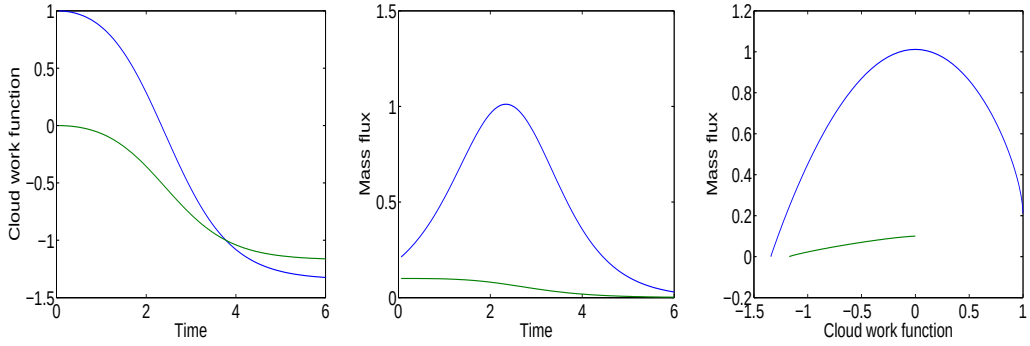

Figure 16: Example solution for the unforced $p = 1$ system with parameters chosen to violate the initial periodicity condition, and with $r_c < 0$. Blue is for the deep mode and green for the shallow mode. The parameters are the default set described in Section 3.2, giving scaling factors of $A_{d0} = 10$ Jkg^{-1}, $A_{s0} = 1$ Jkg^{-1}, $M_{d0} = 5 \times 10^{-3}$ kgm^{-2}s^{-1}, $M_{s0} = 10^{-2}$ kgm^{-2}s^{-1} and $\tau_s = \tau_d = 10^3$ s. The initial conditions are $x_d(0) = 0.2$, $x_s(0) = 0.1$, $y_d(0) = 1$ and $y_s(0) = 0$ so that $r_c = -0.5$. Shown in the same format as in Fig. 12.

be obtained by first substituting for x_s from Eq. 5.5.1 into Eq. 5.3.1d to obtain a differential equation containing x_d and y_d. Combining that with Eq. 5.3.1b we can then eliminate the time to obtain a differential equation connecting x_d and y_d. Integrating the resulting equation produces

$$\frac{\mu y_d^2}{2} + x_d - \frac{\hat{\beta}_s}{q} x_s(0) \left(\frac{x_d}{x_d(0)} \right)^q = \frac{\mu y_d(0)^2}{2} + x_d(0) - \frac{\hat{\beta}_s}{q} x_s(0). \qquad (5.5.2)$$

Similarly it is straightforward to find the solution path in the shallow part of phase space to be

$$\frac{y_s^2}{2} - x_s + \hat{\beta}_d q x_d(0) \left(\frac{x_s}{x_s(0)} \right)^{1/q} = \frac{y_s(0)^2}{2} - x_s(0) + \hat{\beta}_d q x_d(0). \qquad (5.5.3)$$

Together Eqs. 5.5.1, 5.5.2 and 5.5.3 describe the complete solution in

phase space. In order to examine the form of that solution we consider below the phase space of the deep variables. An analysis in terms of shallow variables can be performed along very similar lines and is entirely consistent with the conclusions reached below.

Let us first define a function

$$X_d(x_d) = x_d - \frac{\hat{\beta}_s}{q} x_s(0) \left(\frac{x_d}{x_d(0)} \right)^q \tag{5.5.4}$$

and a constant

$$u_d = \mu \frac{y_d(0)^2}{2} + x_d(0) - \frac{\hat{\beta}_s}{q} x_s(0) \tag{5.5.5}$$

so that Eq. 5.5.2 reads

$$\mu \frac{y_d^2}{2} + X_d(x_d) = u_d. \tag{5.5.6}$$

Note that X_d is bounded from above by u_d. An extreme value for X_d occurs at

$$x_d^{\text{ex}} = \left(\frac{x_d(0)^q}{\hat{\beta}_s x_s(0)} \right)^{1/(q-1)} \tag{5.5.7}$$

at which point

$$X_d(x_d^{\text{ex}}) = \left(1 - \frac{1}{q} \right) \left[\frac{x_d(0)^q}{\hat{\beta}_s x_s(0)} \right]^{1/(q-1)}. \tag{5.5.8}$$

To see what kind of extreme value this is, we can look at the second derivative,

$$\frac{d^2 X_d}{dx_d^2} = -(q-1) \frac{\hat{\beta}_s x_s(0) x_d^{q-2}}{x_d(0)^q}. \tag{5.5.9}$$

Thus, the form of the solution depends on q, with three possibilities to be considered in turn in the following three subsections (Fig. 17): $q > 1$ in which case X_d has a maximum, $q = 1$ in which case X_d is unbounded, and $q < 1$ in which case X_d has a minimum. From Eq. 5.5.6 we immediately notice that for y_d^2 to be bounded then X_d must have a minimum. Thus, if $q < 1$ we

ensure a solution that cannot explode. Examples and further discussions are given below.

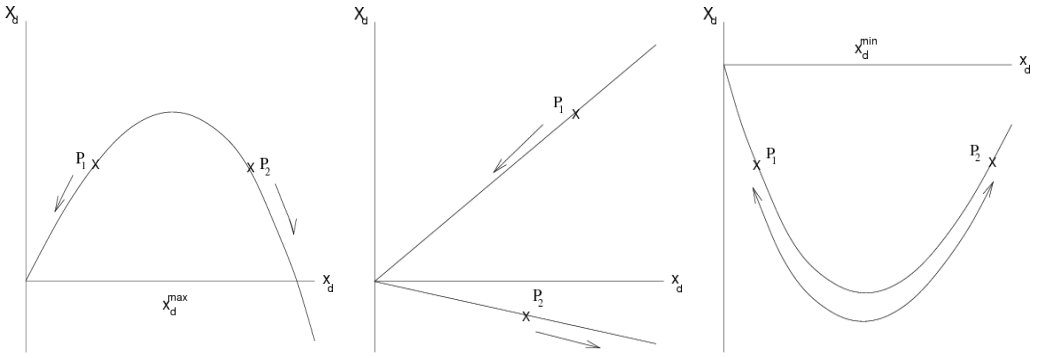

Figure 17: Sketch of the function $X_d(x_d)$ for (left) $q > 1$, (center) $q = 1$ and (right) $q < 1$.

5.5.1. Form of solution for $q > 1$

If $q > 1$ then X_d has a maximum at a positive value of X_d as sketched in Fig. 17 (on the left). Consider the point P at which $y_d = 0$ in the space of (x_d, X_d). Here X_d takes the largest value that could be obtained in an actual solution of Eq. 5.5.6, with $X_d(x_d) = u_d$. This point could correspond to the maximum possible value of the function $X_d(x_d)$ as determined above, but more likely is that there are two possible solutions for $X_d(x_d) = u_d$ on either side of that maximum. We label those points as P_1 and P_2 on the left and right of the maximum respectively. Which side of the $X_d(x_d)$ curve an actual solution begins will depend upon the initial conditions.

Suppose that we are initially on the left-hand branch of the curve (*i.e.*, if $x_d(0) < x_d^{\rm ex}$). Any value of $y_d \neq 0$ that occurs in the solution must correspond to a smaller value of x_d compared to that at P_1. This means

that the solution can only occupy the region between P_1 and the origin, thus including the possibilty of $x_d \to 0$ (and also $x_s \to 0$) so that all convective activity dies out. Fig. 18 illustrates a numerical solution.

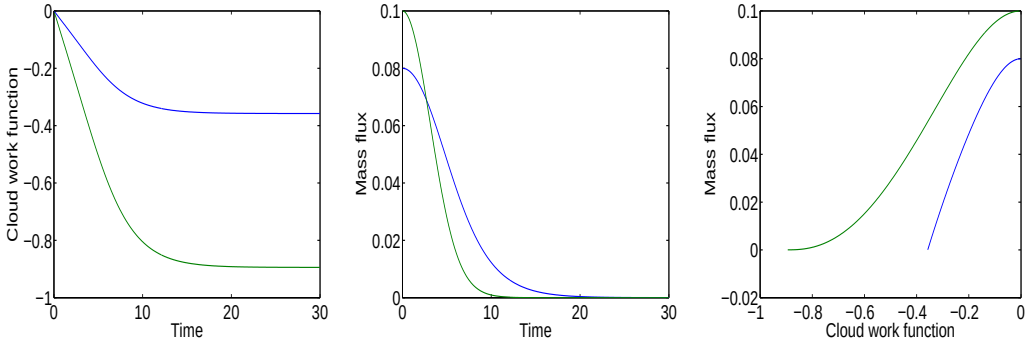

Figure 18: Example solution for the unforced $p = 1$ system with $q > 1$, a damping case. Blue is for the deep mode and green for the shallow mode. The parameters are the default set described in Section 3.2 except for $\alpha_d = 5 \times 10^4$ m^2 s^{-1}, giving scaling factors of $A_{d0} = 50$ Jkg^{-1}, $A_{s0} = 1$ Jkg^{-1}, $M_{d0} = 2.5 \times 10^{-2}$ kgm^{-2}s^{-1}, $M_{s0} = 10^{-2}$ kgm^{-2}s^{-1} and $\tau_s = \tau_d = 10^3$ s. The parameter $q = 2.5$. The initial conditions are $x_d(0) = 0.08$, $x_s(0) = 0.1$, $y_d(0) = 0$ and $y_s(0) = 0$ so that $r_c = 0$. The maximum of $X_d(x_d)$ occurs for $x_d^{\rm ex} = 0.127$. Shown in the same format as in Fig. 12.

Otherwise the initial state will be on the right-hand branch of the $X_d(x_d)$ curve (*i.e.*, with $x_d(0) > x_d^{\rm ex}$). In that case any value of $y_d \neq 0$ that occurs in the solution must correspond to a larger value of x_d compared to that at P_2. This means that the solution occupies a region between P_2 and a point where $x_d \to \infty$ (and also $x_s \to \infty$). Thus the system is able to explode. Fig. 19 illustrates a numerical solution for this case.

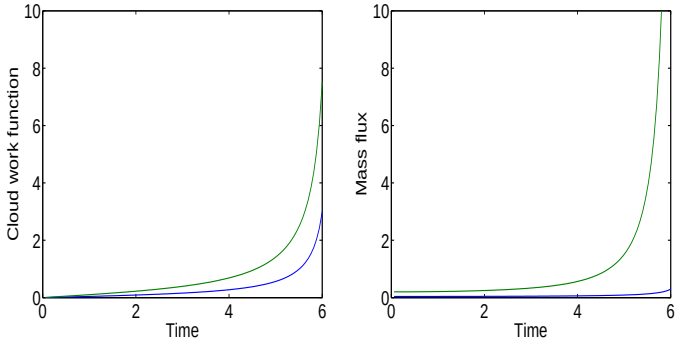

Figure 19: Example solution for the unforced $p = 1$ system with $q > 1$, an exploding case. Blue is for the deep mode and green for the shallow mode. The parameters are the default set described in Section 3.2 except for $\alpha_d = 5 \times 10^4$ m^2 s^{-1}, giving scaling factors of $A_{d0} = 50$ Jkg^{-1}, $A_{s0} = 1$ Jkg^{-1}, $M_{d0} = 2.5 \times 10^{-2}$ kgm^{-2}s^{-1}, $M_{s0} = 10^{-2}$ kgm^{-2}s^{-1} and $\tau_s = \tau_d = 10^3$ s. The parameter $q = 2.5$. The initial conditions are $x_d(0) = 0.04$, $x_s(0) = 0.1$, $y_d(0) = 0$ and $y_s(0) = 0$ so that $r_c = 0$. The maximum of $X_d(x_d)$ occurs for $x_d^{\rm ex} = 0.025$. Shown in the same format as in Fig. 11.

5.5.2. Form of solution for $q = 1$

If $q = 1$ then X_d becomes simply proportional to x_d and so the function does not have any extreme values. A sketch of the situation can be seen in Fig. 17 (in the centre). Specifically, we have

$$X_d = x_d \left[1 - \frac{\hat{\beta}_s}{q} \frac{x_s(0)}{x_d(0)} \right] \tag{5.5.10}$$

According to the sign of the factor in square brackets, X_d is a straight line through the origin with either positive or negative gradient.

Consider the case of a positive gradient (*i.e.*, if $q x_d(0) > \hat{\beta}_s x_s(0)$) and a point P_1 in the space of (x_d, X_d) at which $y_d = 0$ and so $X_d(x_d) = u_d$. This is the largest value of X_d that can be obtained in an actual solution and any

other value of y_d that occurs must therefore correspond to a smaller value of x_d compared to that at P_1. This means that the solution can reach a situation where $x_d \to 0$ (and also $x_s \to 0$) so that all convective activity dies out. Fig. 20 illustrates this case numerically.

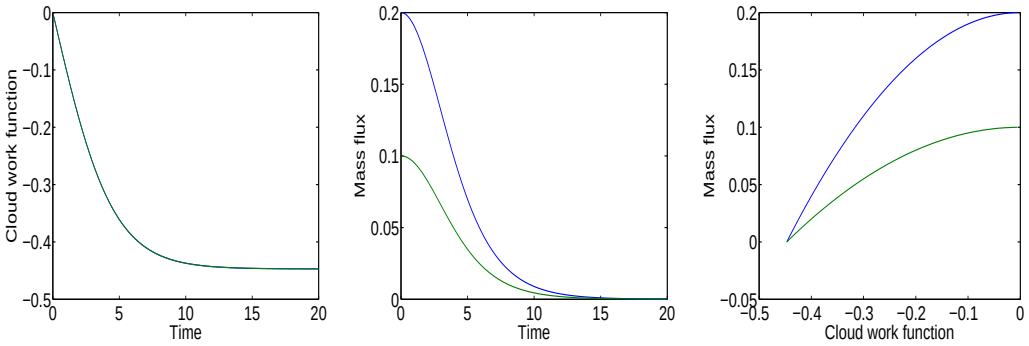

Figure 20: Example solution for the unforced $p = 1$ system with $q = 1$, a damping case. Blue is for the deep mode and green for the shallow mode. The parameters are the default set described in Section 3.2 except for $\alpha_d = 2 \times 10^4$ m^2 s^{-1}, giving scaling factors of $A_{d0} = 20$ Jkg^{-1}, $A_{s0} = 1$ Jkg^{-1}, $M_{d0} = 10^{-2}$ kgm^{-2}s^{-1}, $M_{s0} = 10^{-2}$ kgm^{-2}s^{-1} and $\tau_s = \tau_d = 10^3$ s. The initial conditions are $x_d(0) = 0.2$, $x_s(0) = 0.1$, $y_d(0) = 0$ and $y_s(0) = 0$ so that $r_c = 0$, and the two cloud work functions are equal at all times. Shown in the same format as in Fig. 12.

For the case of a negative gradient, we consider a point P_2, again defined by $y_d = 0$ and $X_d(x_d) = u_d$. In this case any other value of y_d that occurs in the solution must make X_d more negative and must therefore correspond to a larger value of x_d compared to that at P_2. Thus the system is able to explode. Fig. 21 illustrates this case numerically.

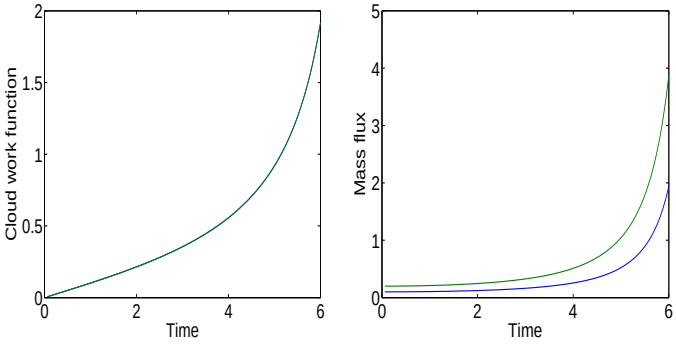

Figure 21: Example solution for the unforced $p = 1$ system with $q = 1$, an exploding case. Blue is for the deep mode and green for the shallow mode. The parameters are the default set described in Section 3.2 except for $\alpha_d = 2 \times 10^4$ m^2 s^{-1}, giving scaling factors of $A_{d0} = 20$ Jkg^{-1}, $A_{s0} = 1$ Jkg^{-1}, $M_{d0} = 10^{-2}$ kgm^{-2}s^{-1}, $M_{s0} = 10^{-2}$ kgm^{-2}s^{-1} and $\tau_s = \tau_d = 10^3$ s. The initial conditions are $x_d(0) = 0.1$, $x_s(0) = 0.2$, $y_d(0) = 0$ and $y_s(0) = 0$ so that $r_c = 0$, and the two cloud work functions are equal at all times. Shown in the same format as in Fig. 11.

5.5.3. Form of solution for $q < 1$

If $q < 1$ then X_d has a minimum at a negative value of X_d. A sketch of the situation can be seen in Fig. 17 (on the right). Once again we consider a point P in the space of (x_d, X_d) given by $y_d = 0$ and hence $X_d(x_d) = u_d$. The point could correspond to the minimum of the function $X_d(x_d)$ as derived above, but more likely is that there are two possible solutions for P on either side of that minimum. We label those points as P_1 and P_2 on the left and right of the minimum respectively.

Suppose that the initial conditions place us on the left–hand branch of the curve (*i.e.*, if $x_d(0) < x_d^{\rm ex}$). Any non-zero value of y_d that occurs in the

solution must correspond to a larger value of x_d compared to that at P_1. This means that the solution is able to access the right–hand branch of the curve although it cannot go beyond the point P_2 itself because there are no values of y_d that could allow it. Similarly for initial conditions on the right–hand branch of the curve, the solution is able to access the left–hand branch, although of course we cannot go past the point P_1. Fig. 22 illustrates the periodic solution that is found numerically for $q < 1$.

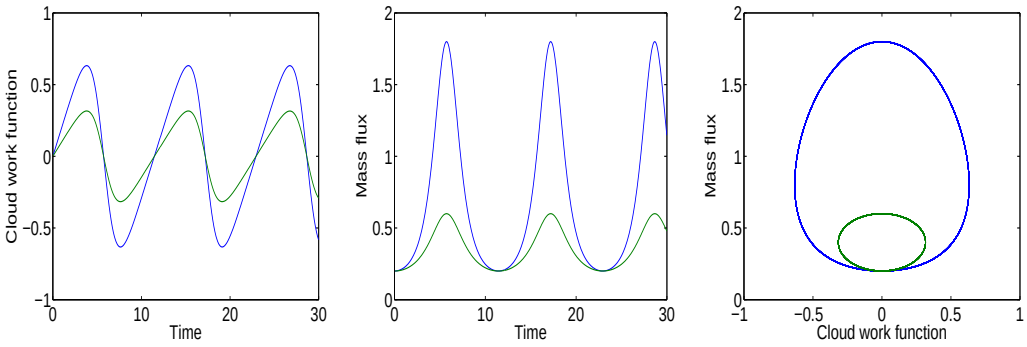

Figure 22: Example solution for the unforced $p = 1$ system with $q < 1$. Blue is for the deep mode and green for the shallow mode. The parameters are the default set described in Section 3.2, giving scaling factors of $A_{d0} = 20$ Jkg^{-1}, $A_{s0} = 1$ Jkg^{-1}, $M_{d0} = 10^{-2}$ kgm^{-2}s^{-1}, $M_{s0} = 10^{-2}$ kgm^{-2}s^{-1} and $\tau_s = \tau_d = 10^3$ s. The initial conditions are $x_d(0) = 0.2$, $x_s(0) = 0.2$, $y_d(0) = 0$ and $y_s(0) = 0$ so that $r_c = 0$. The parameter $q = 0.5$. Shown in the same format as in Fig. 12.

5.6. Linearization of the $p = 1$ system

The $p = 1$ system is fully nonlinear as emphasized by Yano and Plant (2012a) for the one–mode case. It is nonetheless revealing to consider linearized analyses in order to show the evolution in the vicinity of various

situations of particular physical interest. Important questions concern the behaviour of the system when it deviates slightly from the full set of conditions for periodicity that were determined in Sections 5.3 to 5.5. After presenting a linear formulation in Section 5.6.1 below, we then consider a range of special cases in turn.

5.6.1. General approach for linearization with vanishing determinant

Consider a linearization of the coupled $p = 1$ system about an arbitrary reference state, which we denote with the subscript r. Using a prime to denote a departure from the reference state the linearized form of Eqs. 5.3.1a to 5.3.1d is:

$$\dot{x}'_s = x_{sr} y'_s + y_{sr} x'_s \tag{5.6.1a}$$

$$\dot{x}'_d = \mu(x_{dr} y'_d + y_{dr} x'_d) \tag{5.6.1b}$$

$$\dot{y}'_s = x_{sr} - \hat{\beta}_d x_{dr} + x'_s - \hat{\beta}_d x'_d \tag{5.6.1c}$$

$$\dot{y}'_d = -x_{dr} + \hat{\beta}_s x_{sr} - x'_d + \hat{\beta}_s x'_s. \tag{5.6.1d}$$

We specialize to reference states that satisfy

$$x_{sr} = \hat{\beta}_d x_{dr} \tag{5.6.2a}$$

$$x_{dr} = \hat{\beta}_s x_{sr}. \tag{5.6.2b}$$

The combination of these two constraints means that $\hat{\beta}_s \hat{\beta}_d = 1$ and so we are dealing with a vanishing determinant as discussed in Section 5.3. This means that the cloud–work functions are linked by Eq. 5.3.3, and by furthermore taking the initial state to be the reference state this reads

$$y'_s = \hat{\beta}_d y'_d. \tag{5.6.3}$$

Since the above relation must be satisfied at all times, this includes the initial time, and so the reference state must itself satisfy the initial periodicity condition,

$$y_{sr} = \hat{\beta}_d y_{dr}. \tag{5.6.4}$$

Although this constraint and Eq. 5.6.2a mean that reference state is not arbitrary it should be recognized that there is still considerable freedom remaining in its choice. Using Eq. 5.6.3 to eliminate y'_d, Eqs. 5.6.1a to 5.6.1c become

$$\left(\frac{d}{dt} - y_{sr}\right) x'_s = x_{sr} y'_s \tag{5.6.5a}$$

$$\left(\frac{d}{dt} - \frac{y_{sr}}{q}\right) x'_d = \frac{x_{sr}}{\mu q^2} y'_s \tag{5.6.5b}$$

$$\dot{y}'_s = x'_s - \mu q x'_d \tag{5.6.5c}$$

where we have also made use of Eqs. 5.6.2a and 5.6.3 to eliminate x_{dr} and y_{dr} respectively and have expressed the final result using the parameter q defined in Eq. 5.4.4. From the above equations we can now easily derive an eigenvalue equation. Specifically, Eq. 5.6.5c gives

$$\sigma y'_s = x'_s - \mu q x'_d \tag{5.6.6}$$

using which we can eliminate y'_s in Eqs. 5.6.5a and 5.6.5b to produce

$$\left[\sigma(\sigma - y_{sr}) - x_{sr}\right] x'_s + \mu q x_{sr} x'_d = 0 \tag{5.6.7}$$

and

$$\left[\sigma\left(\sigma - \frac{y_{sr}}{q}\right) + \frac{x_{sr}}{q}\right] x'_d - \frac{x_{sr}}{\mu q^2} x'_s = 0 \tag{5.6.8}$$

respectively. Now by taking the determinant of the above two equations, we obtain the eigenvalue equation

$$\sigma^2 - \frac{y_{sr}}{q}(1+q)\sigma + \frac{1}{q}\left(x_{sr}(1-q) + y_{sr}^2\right) = 0. \tag{5.6.9}$$

This gives the eigenvalues for a linearization of the coupled $p = 1$ system about an initial reference state for which the conditions 5.6.2a and 5.6.2b hold. We consider two particular choices of reference state in the next two subsections.

5.6.2. Reference state 1: Linearization about zero mass flux

For a linearization about zero mass flux we set $x_{sr} = x_{dr} = 0$ so that the eigenvalue equation 5.6.9 becomes

$$\sigma^2 - \frac{y_{sr}}{q}(1+q)\sigma + \frac{1}{q}y_{sr}^2 = 0 \tag{5.6.10}$$

with roots $\sigma = y_{sr}$ and y_{sr}/q. Thus, convection will either grow or decay according to the sign of the nondimensionalized cloud work function. The result accords with the physical expectation that from an initial state of zero mass flux then excess of cloud work function beyond its equilibrium value will lead to the growth of convection, whereas a value below equilibrium will produce decay of any linear fluctuation.

Figs. 23 and 24 show example results for this approximation with y_{sr} positive and negative respectively. The plots include the solution obtained from the fully nonlinear equations as well as that from the linearized equation set. The two solutions agree very well, up to $t \sim 3\tau_s$ in the growing case and at all times in the decaying case.

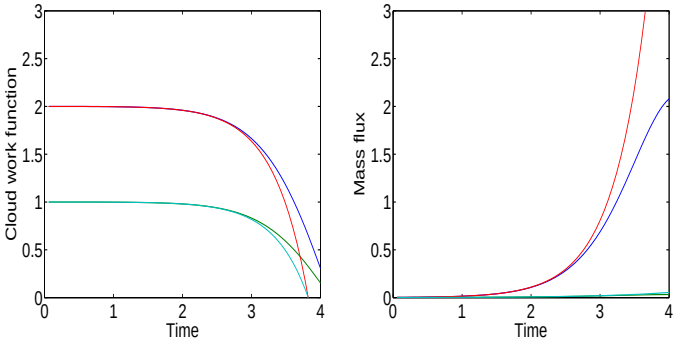

Figure 23: Example solution for a linearized approximation of the unforced $p = 1$ system. The linearization is about a state of zero mass flux and y_{sr} is positive. The parameters are the default set described in Section 3.2, giving scaling factors of $A_{d0} = 20$ Jkg^{-1}, $A_{s0} = 1$ Jkg^{-1}, $M_{d0} = 10^{-2}$ kgm^{-2}s^{-1}, $M_{s0} = 10^{-2}$ kgm^{-2}s^{-1} and $\tau_s = \tau_d = 10^3$ s. The initial conditions are $x_d(0) = 2 \times 10^{-3}$, $x_s(0) = 10^{-3}$, $y_d(0) = 2$ and $y_s(0) = 1$. Blue is for the deep mode and green for the shallow mode using the fully nonlinear equations. Red is for the deep mode and cyan for the shallow mode using the linearized equations. Shown in the same format as in Fig. 11.

5.6.3. Reference state 2: Linearization about cloud work function equilibrium

Equilibrium of the mass flux tendency equations, 5.3.1a and 5.3.1b, occurs when the cloud work functions are $y_s = y_d = 0$. Linearizing about that state reduces the eigenvalue equation 5.6.9 to

$$\sigma^2 = \left(\frac{q-1}{q} \right) x_{sr}. \tag{5.6.11}$$

Thus, a linear perturbation about the cloud work function equilibrium state is exponentially growing for $q > 1$ and oscillatory for $q < 1$, consistent with the nonlinear analysis of Section 5.5. Figs. 25 and 26 show example results for this linear regime with $q > 1$ and $q < 1$ respectively.

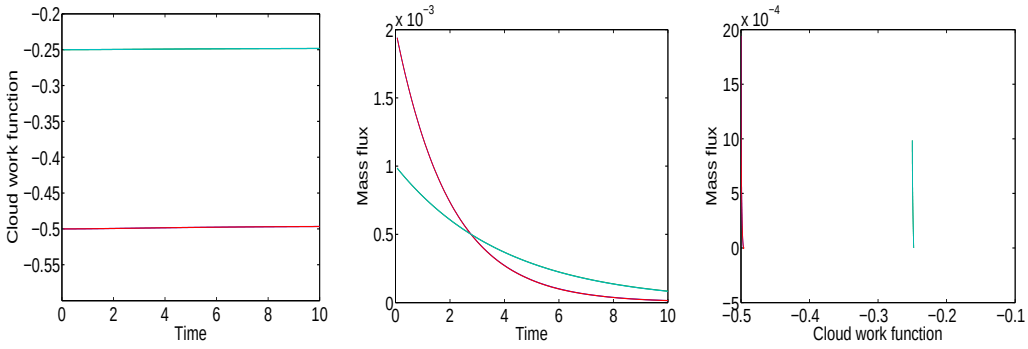

Figure 24: Example solution for a linearized approximation of the unforced $p = 1$ system. The linearization is about a state of zero mass flux and y_{sr} is negative. The parameters are the default set described in Section 3.2, giving scaling factors of $A_{d0} = 20$ Jkg^{-1}, $A_{s0} = 1$ Jkg^{-1}, $M_{d0} = 10^{-2}$ kgm^{-2}s^{-1}, $M_{s0} = 10^{-2}$ kgm^{-2}s^{-1} and $\tau_s = \tau_d = 10^3$ s . The initial conditions are $x_d(0) = 2 \times 10^{-3}$, $x_s(0) = 10^{-3}$, $y_d(0) = -0.5$ and $y_s(0) = -0.25$. Blue is for the deep mode and green for the shallow mode using the fully nonlinear equations. Red is for the deep mode and with cyan for the shallow mode using the linearized equations. Shown in the same format as in Fig. 12. Differences between the linear and nonlinear solutions are almost imperceptible in this case as the linear solutions provide a very good approximation.

An interesting point to notice is that the square of the oscillation frequency (assuming $q < 1$) is proportional to the reference/initial state mass flux, here written in terms of shallow convection. Thus, the period of oscillation could be arbitrarily increased by decreasing the initial amplitude of convective activity. In principle, the oscillation period could even be extended to an MJO timescale.

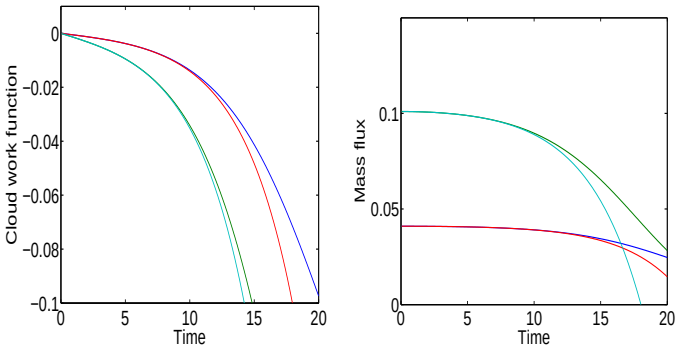

Figure 25: Example solution for a linearized approximation of the unforced $p = 1$ system. The linearization is about a state of cloud work function equilibrium and $q > 1$. The parameters are the default set described in Section 3.2, except for $\alpha_d = 5 \times 10^{-4}\mathrm{m}^2\mathrm{s}^{-1}$, giving scaling factors of $A_{d0} = 50$ Jkg^{-1}, $A_{s0} = 1$ Jkg^{-1}, $M_{d0} = 2.5 \times 10^{-2}$ $\mathrm{kgm}^{-2}\mathrm{s}^{-1}$, $M_{s0} = 10^{-2}$ $\mathrm{kgm}^{-2}\mathrm{s}^{-1}$ and $\tau_s = \tau_d = 10^3$ s. The parameter $q = 2.5$. The initial conditions are $x_d(0) = 0.041$, $x_s(0) = 0.101$, $y_d(0) = 0$ and $y_s(0) = 0$. Blue is for the deep mode and green for the shallow mode using the fully nonlinear equations. Red is for the deep mode and cyan for the shallow mode using the linearized equations and a reference state of $x_{sr} = 0.04$, $x_{dr} = 0.1$, $y_{sr} = y_{dr} = 0$. Shown in the same format as in Fig. 11.

5.6.4. Linearization with a timescale separation

The above numerical examples were for cases where $\tau_s = \tau_d$ ($\mu = 1$) and showed that the linearized equations are able to give a good approximation to the full system, at least for times t of order a few τ_s. However, it should be noted that a linearization works less well if there is a timescale separation.

Suppose first that shallow convection is damped very slowly compared to deep convection so that $\tau_s \gg \tau_d$, or $\mu \gg 1$. In this limit shallow convection dominates and the system quickly comes to resemble the shallow-only regime which is markedly nonlinear. Longer integrations with $q < 1$ confirm that

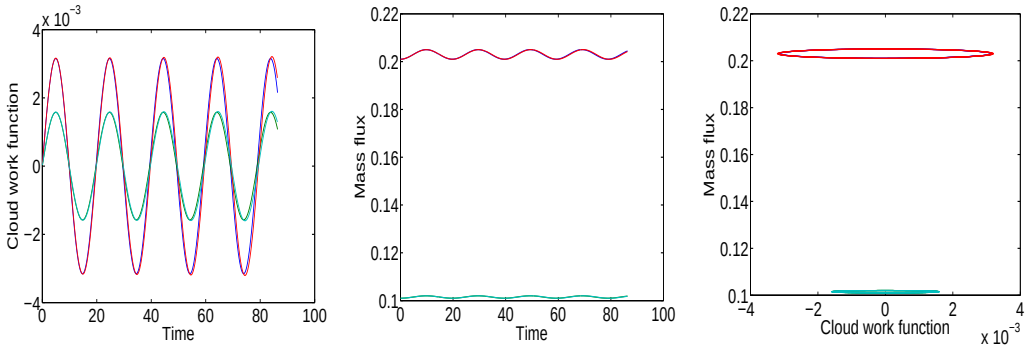

Figure 26: Example solution for a linearized approximation of the unforced $p = 1$ system. The linearization is about a state of cloud work function equilibrium and $q < 1$. The parameters are the default set described in Section 3.2, giving scaling factors of $A_{d0} = 20$ Jkg^{-1}, $A_{s0} = 1$ Jkg^{-1}, $M_{d0} = 10^{-2}$ kgm^{-2}s^{-1}, $M_{s0} = 10^{-2}$ kgm^{-2}s^{-1} and $\tau_s = \tau_d = 10^3$ s. The parameter $q = 0.5$. The initial conditions are $x_d(0) = 0.201$, $x_s(0) = 0.101$, $y_d(0) = 0$ and $y_s(0) = 0$. Blue is for the deep mode and green for the shallow mode using the fully nonlinear equations. Red is for the deep mode and with cyan for the shallow mode using the linearized equations and a reference state of $x_{sr} = 0.1$, $x_{dr} = 0.2$, $y_{sr} = y_{dr} = 0$. Shown in the same format as in Fig. 12. Differences between the linear and nonlinear solutions are almost imperceptible in this case as the linear solutions provide a very good approximation.

deep convection can tame this growth tendency and produce the oscillating solution expected but such behaviour is only apparent for the full nonlinear system. Fig. 27 illustrates these points.

In the opposite limit of $\mu \ll 1$ shallow convection is rapidly damped compared to deep convection. Here again, numerical tests of the linearized system perform relatively poorly. Fig. 28 gives an illustration. In order for linearity to be a good approximation we require the deep and shallow

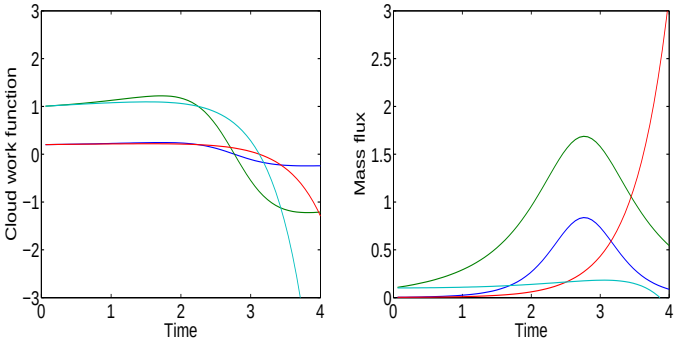

Figure 27: Example solution for a linearized approximation of the unforced $p = 1$ system, with a timescale separation so that $\mu \gg 1$. The parameters are the default set described in Section 3.2, except for $\tau_d = 100$ s, giving scaling factors of $A_{d0} = 100$ Jkg^{-1}, $A_{s0} = 1$ Jkg^{-1}, $M_{d0} = 5 \times 10^{-2}$ kgm^{-2}s^{-1}, $M_{s0} = 10^{-2}$ kgm^{-2}s^{-1} and $\tau_s = 10^3$ s. The parameter $q = 0.5$. The initial conditions are $x_d(0) = 0.003$, $x_s(0) = 0.101$, $y_d(0) = 0.2$ and $y_s(0) = 1$. Blue is for the deep mode and green for the shallow mode using the fully nonlinear equations. Red is for the deep mode and cyan for the shallow mode using the linearized equations and a reference state of $x_{sr} = 0.1$, $x_{dr} = 0.001$, $y_{sr} = 1$ and $y_{dr} = 0.2$. Shown in the same format as in Fig. 11.

modes to be well balanced at all times, while the fully nonlinear equation set is needed to handle a situation where one of the modes dominates the short–time but not long–time dynamics.

5.7. Linearization for the case of a non-zero determinant

We now return to the linearized equations 5.6.1a to 5.6.1d but develop these in a different way. In Section 5.6.1 we specialized to reference states satisfying Eqs. 5.6.2a and 5.6.2b, thereby requiring a vanishing determinant. The purpose of the present subsection is to make a linear expansion for a non-

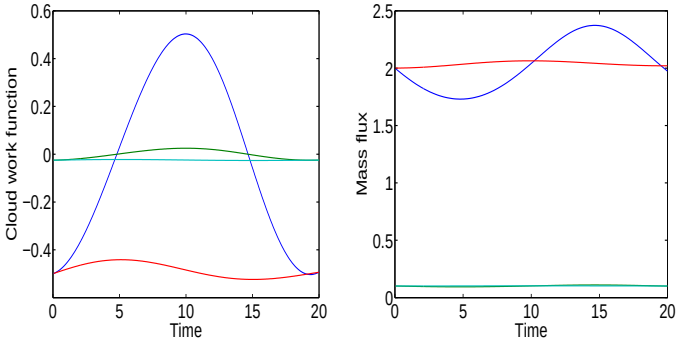

Figure 28: Example solution for a linearized approximation of the unforced $p = 1$ system, with a timescale separation so that $\mu \ll 1$. The parameters are the default set described in Section 3.2, except for $\tau_d = 10^4$ s, giving scaling factors of $A_{d0} = 1$ Jkg^{-1}, $A_{s0} = 1$ Jkg^{-1}, $M_{d0} = 5 \times 10^{-4}$ kgm^{-2}s^{-1}, $M_{s0} = 10^{-2}$ kgm^{-2}s^{-1} and $\tau_s = 10^3$ s. The parameter $q = 0.5$. The initial conditions are $x_d(0) = 2.001$, $x_s(0) = 0.101$, $y_d(0) = -0.5$ and $y_s(0) = -0.025$. Blue is for the deep mode and green for the shallow mode using the fully nonlinear equations. Red is for the deep mode and cyan for the shallow mode using the linearized equations and a reference state of $x_{sr} = 0.1$, $x_{dr} = 2$, $y_{sr} = -0.025$ and $y_{dr} = -0.5$. Shown in the same format as in Fig. 11.

zero determinant. We do however constrain the reference states of interest by linearizing about the equilibrium values of the cloud work function so that $y_{sr} = y_{dr} = 0$.

The linearized equations for this situation read as follows.

$$\dot{x}'_s = x_{sr} y'_s \tag{5.7.1a}$$

$$\dot{x}'_d = \mu x_{dr} y'_d \tag{5.7.1b}$$

$$\dot{y}'_s = x_{sr} - \hat{\beta}_d x_{dr} + x'_s - \hat{\beta}_d x'_d \tag{5.7.1c}$$

$$\dot{y}'_d = -x_{dr} + \hat{\beta}_s x_{sr} - x'_d + \hat{\beta}_s x'_s \tag{5.7.1d}$$

Taking a time derivative of Eqs. 5.7.1c, d and then using Eqs. 5.7.1a, b to eliminate $\dot{x}'_s$ and $\dot{x}'_d$ we find that

$$\ddot{y}'_s - x_{sr}y'_s + \hat{\beta}_d \mu x_{dr} y'_d = 0 \tag{5.7.2a}$$

$$\ddot{y}'_d + \mu x_{dr} y'_d - \hat{\beta}_s x_{sr} y'_s = 0. \tag{5.7.2b}$$

It is then straightforward to obtain the eigenvalue equation

$$(\sigma^2 - x_{sr})(\sigma^2 + \mu x_{dr}) + \mu \hat{\beta}_d \hat{\beta}_s x_{sr} x_{dr} = 0$$

or

$$\sigma^4 + (\mu x_{dr} - x_{sr})\sigma^2 + (\hat{\beta}_s \hat{\beta}_d - 1)\mu x_{sr} x_{dr} = 0. \tag{5.7.3}$$

The solution may be written as

$$\sigma^2 = \frac{\sigma_0^2}{2}\left(1 \pm (1-\lambda)^{1/2}\right) \tag{5.7.4}$$

where we have defined

$$\sigma_0^2 = x_{sr} - \mu x_{dr} \tag{5.7.5}$$

$$\lambda = \frac{4(\hat{\beta}_s \hat{\beta}_d - 1)\mu x_{sr} x_{dr}}{\sigma_0^4}. \tag{5.7.6}$$

The behaviour depends on the initial mass flux difference between shallow and deep convection, as measured by σ_0^2, and on the departure from a vanishing determinant, as measured by λ.

If $\lambda \leq 1$ then σ^2 is purely real and is either positive or negative in accordance with the sign of σ_0^2. Thus, there are purely oscillatory modes for $\sigma_0^2 < 0$ (deep convection dominates in the initial state) or both growing and decaying modes for $\sigma_0^2 > 0$ (shallow convection dominates in the initial state). The other possibility is that $\lambda > 1$ and so σ^2 is complex. In that case there are both decaying and growing oscillatory modes regardless of the sign of σ_0^2.

Most of these cases contain a growing mode indicating that most values for the convective mass fluxes are unstable even when the system is started from the cloud work function equilibrium. A numerical example is shown in Fig. 29. The exception occurs for $\sigma_0^2 < 0$ and $\lambda \leq 1$ in which case the solution is periodic in the linear regime, although this is no longer true in a fully nonlinear regime. The numerical example in Fig. 30 illustrates such a case, in which the linearized system is periodic but for which all convective activity is damped out in the nonlinear regime. The linear approximation breaks down relatively quickly for this case, at $t \sim 0.5\tau_s$.

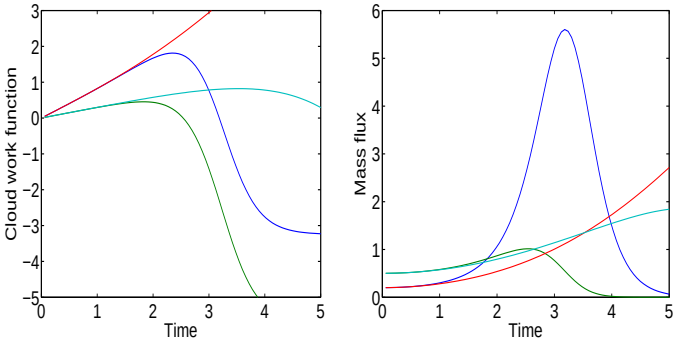

Figure 29: Example solution for a linearized approximation of the unforced $p = 1$ system with finite determinant; here for a growing case in the linear regime with $\sigma_0^2 = 0.3$ and $\lambda = 4.4$. The parameters are the default set described in Section 3.2, except for $\beta_d = 0.2$ Jm^{2}kg^{-2}, giving scaling factors of $A_{d0} = 10$ Jkg^{-1}, $A_{s0} = 1$ Jkg^{-1}, $M_{d0} = 5 \times 10^{-3}$ kgm^{-2}s^{-1}, $M_{s0} = 10^{-2}$ kgm^{-2}s^{-1} and $\tau_s = \tau_d = 10^3$ s. The initial conditions are $x_d(0) = 0.201$, $x_s(0) = 0.501$, $y_d(0) = 0$ and $y_s(0) = 0$. Blue is for the deep mode and green for the shallow mode using the fully nonlinear equations. Red is for the deep mode and cyan for the shallow mode using the linearized equations and a reference state of $x_{sr} = 0.5$, $x_{dr} = 0.2$, $y_{sr} = y_{dr} = 0$. Shown in the same format as in Fig. 11.

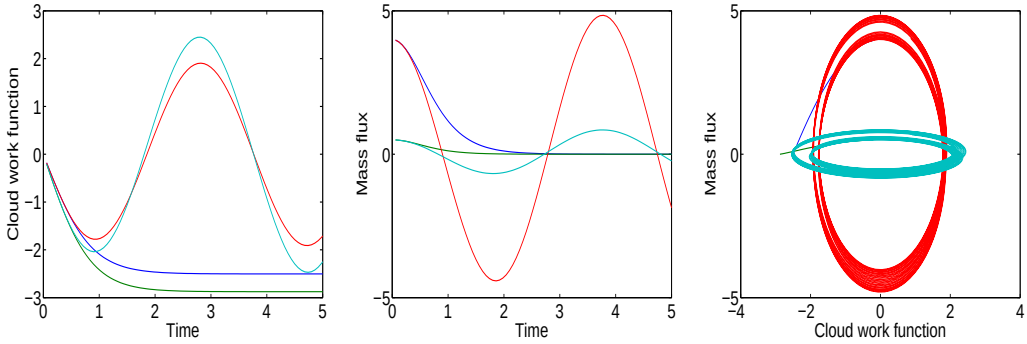

Figure 30: Example solution for a linaerzied approximation of the unforced $p = 1$ system with finite determinant; here for an oscillating case in the linear regime with $\sigma_0^2 = -3.5$ and $\lambda = 0.65$. The parameters are the default set described in Section 3.2, excep for $\beta_d = 0.2$ Jm^{2}kg^{-2}, giving scaling factors of $A_{d0} = 10$ Jkg^{-1}, $A_{s0} = 1$ Jkg^{-1}, $M_{d0} = 5 \times 10^{-3}$ kgm^{-2}s^{-1}, $M_{s0} = 10^{-2}$ kgm^{-2}s^{-1} and $\tau_s = \tau_d = 10^3$ s. The initial conditions are $x_d(0) = 4.001$, $x_s(0) = 0.501$, $y_d(0) = 0$ and $y_s(0) = 0$. Blue is for the deep mode and green for the shallow mode using the fully nonlinear equations. Red is for the deep mode and cyan for the shallow mode using the linearized equations and a reference state of $x_{sr} = 0.5$, $x_{dr} = 4$, $y_{sr} = y_{dr} = 0$. Shown in the same format as in Fig. 12.

5.8. Summary of results for the $p = 1$ system

The system of Eqs. 5.0.1 and 5.0.2 arises from Arakawa and Schubert's (1974) energy cycle description for a system with two types of convection, along with Yano and Plant's (2012a) linear assumption for the relationship between convective kinetic energy and cloud–base mass flux. All of the parameters in those equations are assumed to be positive in accordance with the arguments presented in Section 2.

The main points arising from our analysis of the system are:

- The stability of the unforced shallow system in isolation depends on

the initial conditions (Section 5.1), specifically the combination $r_s^2 \equiv y_s(0)^2 - 2x_s(0)$. For $r_s^2 < 0$ the system explodes, for $r_s^2 = 0$ it either becomes infinite at the finite time $t = 2\tau_s/y_s(0)$ (if $y_s(0) > 0$) or else all convection is damped out (if $y_s(0) < 0$), and for $r_s^2 > 0$ then all convection is always damped out. Thus, in contrast to the $p = 2$ system, isolated shallow convection is not necessarily explosive but may decay if the initial mass flux is not too strong. This generalizes the analysis of the Appendix B in Yano and Plant (2012b).

- The unforced deep system in isolation has vanishing convective activity (Section 5.2), regardless of the initial conditions. Thus, it behaves qualitatively like the $p = 2$ system.

- The coupled system may be unstable, damping or neutral according to the parameter settings and the initial conditions. It may also exhibit periodicity. As for the $p = 2$ system, solutions of particular interest are those for which the destablizing and stabilizing tendencies of shallow and deep convection respectively are balanced. A necessary condition for such a solution is that the determinant of the interaction matrix $\mathcal{K}$ should vanish (Section 4.4.1; Eq. 4.4.2).

- The nonlinear $p = 1$ system also has a further requirement on the initial conditions (Section 5.4; Eq. 5.4.3), which we call the initial periodicity condition. The requirement is that $r_c = y_s(0) - \hat{\beta}_d y_d(0) = 0$. If the determinant vanishes but $r_c \neq 0$ then the coupled system aproaches a single-mode system as $t \to \infty$ with shallow (deep) convection dominant for r_c positive (negative).

- Assuming a vanishing determinant and initial periodicity:
  - The shallow and deep convective mass fluxes are linked through a power relationship with power $q = (\beta_d \alpha_d)/(\gamma_d \alpha_s)$ as given in Eq. 5.5.1 of Section 5.5. The qualitative behaviour of the two–mode system is controlled by this power q,
    - For $q > 1$ (Section 5.5.1) either all activity dies out or else the system explodes. Which of these possibilities occurs can be determined from the initial mass flux, which must be smaller than a threshold value for decay (Eq. 5.5.7).
    - For $q = 1$ (Section 5.5.2), the deep and shallow mass fluxes are proportional and again either all activity dies out or else the system explodes. Which of these possibilities occurs can be determined by comparing the initial values of mass flux for deep and shallow convection. Decay occurs if the deep convective mass flux is sufficiently strong that $x_d(0) > \hat{\beta}_s x_s(0)$.
    - For $q < 1$ (Section 5.5.3), the solution is periodic regardless of any further considerations of the initial conditions.
  - We considered a linearization of the equations in order to consider the system with vanishing determinant but with a small departure from initial periodicity. Specifically, we expanded about a reference state that respects initial periodicity (Section 5.6.1).
    - Departures from a reference state of zero mass flux produce growth if the reference cloud work functions are larger than their equilibrium values and decay otherwise (Section 5.6.2).

    - Departures from the equilibrium values of the cloud work functions grow for $q > 1$ and are oscillatory for $q < 1$ (Section 5.6.3).
    - Numerically the linearized solutions provide a good description for $\mu \sim 1$ but perform poorly for $\mu \gg 1$ and $\mu \ll 1$ (Section 5.6.4) in which one mode dominates and non-linear effects are important.
  - We also considered a linearization of the equations in order to explore the case of a non-vanishing determinant with a small departure from equilibrium values of the cloud work functions (Section 5.7). In that case most parameter settings and initial conditions lead to a growing mode increasing the linear departure from the cloud work function equilibrium. However, the departure may be neutral, producing a periodic solution of the linearized equations, if $\sigma_0^2 < 0$ and $\lambda \leq 1$ where σ_0 and λ are defined by Eqs. 5.7.5 and 5.7.6 respectively.

To summarize the above, for most configurations of the $p = 1$ system convection will either decay or explode and the rules above enable us to determine which of these will occur for any given parameter settings and initial conditions. However, the system also supports a bounded periodic solution under the following conditions:

1. The matrix determinant must vanish, $\beta_d \beta_s = \gamma_d \gamma_s$.
2. The forcing must satisfy $F_s = \frac{\gamma_s}{\beta_s} F_d$ which of course includes the case of no forcing.

3. The initial conditions for the cloud work function must satisfy $A_s(0) - A_{s0} = \frac{\gamma_s}{\beta_s}(A_d(0) - A_{d0})$
4. The other parameters of the problem must respect the inequality $q < 1$.

6. Conclusions : Perspectives for Future Studies

The closure of convection parameterization is a long-standing and contentious problem (Yano and Plant, 2012c; Yano et al 2012). The convective energy cycle is an attractive framework for the closure of a mass–flux parameterization, as already attempted by Randall and Pan (1993) and Pan and Randall (1998). Our recent work (Yano and Plant 2012a, b) has proposed modifications to their formulation. Yano and Plant (2012a) proposed to assume that the convective kinetic energy is proportional to the cloud–base mass flux (i.e., $p = 1$ in Eq. 3.1.3) rather than to its square ($p = 2$ in Eq. 3.1.3) as assumed by Randall and Pan (1993) and Pan and Randall (1998). Yano and Plant (2012b), in turn, point out the importance of including the off-diagonal terms of the energy–conversion kernel (i.e., $\mathcal{K}_{i,j} \neq 0$ for $i \neq j$) that are neglected by Randall and Pan (1993) and Pan and Randall (1998), in order to account for the interactions between different convective modes.

These modifications have advantages over the earlier formulation in explaining basic convective processes. A modified functional relationship (modification from $p = 2$ to $p = 1$ in Eq. 3.1.3) leads to a nonlinear term in the coupled ordinary differential equations that makes it possible to explain, under constant large–scale forcing, a life cycle of convective ensembles consisting of discharge and recharge (Yano and Plant 2012a). The introduction of

interactions between different convective modes enables us to explain transformations from shallow to deep convection in a very simple manner (Yano and Plant 2012b).

Our next major goal is to implement this modified energy–cycle formulation into a convection parameterization as a closure that couples both shallow and deep convection schemes. However, in order to make such an implementation and subsequent testing smooth, the stand–alone behaviour of the two-mode energy–cycle system must be well understood. This has been the purpose of the present paper. For this reason, investigations have been performed in a fairly systematic manner for the cases of both $p = 1$ and 2 in Eq. 3.1.3.

The focus has been placed on the two mode case, partly as a reflection of current formulations of convective parameterizations, and partly because two modes are sufficient to produce a rich variety of behaviours. A particular interest here has been conditions for obtaining a perpetual periodic–cycle state under interactions between shallow and deep convection: slow growth of shallow convection triggers deep convection due to its destabilization tendency, and then deep convection suppresses both itself and shallow convection by its stabilization tendency to continue the cycle.

The conditions for such perpetual periodic solutions are carefully sought both for $p = 1$ and 2, because this behaviour is expected to be also important in interpreting global–model behaviours under a practical implementation. A perfect periodic solution is realizable only under a relatively narrow parameter range. However, over a much wider parameter range, the system permits a damped periodic solution under interactions of shallow and deep

modes (see, for example, Figs. 9 and 29). This suggests that the notion of the self–sustaining shallow–deep convection coupled system elucidated by Yano and Plant (2012b) has a wider applicability in practice. We anticipate that various external forcings, which are almost totally neglected in the present study, can induce other cyclic behaviours.

An intriguing feature for the case with $p = 1$ is that the square of the oscillation frequency becomes proportional to a degree of the deviation of the cloud–base mass flux from an equilibrium state. Such freedom for the system to exhibit a periodicity determined by the initial amplitude arises from its nonlinearity. Potentially, even intraseasonal variability may be explained under this framework.

Probably, one more last step before this energy–cycle framework can be introduced as a parameterization closure is to investigate the system under interactions with linear large–scale dynamics. This may even be limited to a horizontally one–dimensional configuration for ease of analysis. Such analysis would provide a more solid understanding of the interactions and implications of the convective energy cycle for tropical dynamics issues, including intraseasonal variability.

Another important extension of the present study is to the case with many convective modes so that the complex mutual interactions of atmospheric moist convection can fully be investigated. Under this extension, the analytic treatment of a small number of coupled ordinary differential equations is no longer sufficient and other approaches to the analysis must be developed, possibly in analogy with those used for statistical mechanics. Thus, the extension opens a way for a new approach to atmospheric convection studies:

statistical cumulus dynamics. This direction has long since been suggested by Arakawa and Schubert (1974) as an ultimate answer for the convection closure problem. The time is now mature for launching full investigations from this perspective.

Appendix A. Dimensional analysis and the functional relation, Eq. 3.1.3

The general functional relation of Eq. 3.1.3 with $p \neq 2$ may at first sight be objected to on dimensional grounds. Dimensional analysis states that the kinetic energy density, k (Jkg^{-1}), can be linked to a characteristic velocity scale, $w_{\rm char}$, through

$$k = \frac{1}{2} w_{\rm char}^2. \tag{A.1}$$

The purpose of this appendix is to show that this standard expression of dimensional analysis does not contradict with Eq. 3.1.3.

The convective kinetic energy, K (Jm^{-2}) appearing in Eq. 2.0.1, is given by

$$K = \int_{z_B}^{z_T} \sigma_c \frac{\rho}{2} w^2 dz \tag{A.2}$$

where w is the vertical velocity in the convective updraft and where attention has been restricted to the vertical component of velocity only, as in Yano and Plant (2012a). All other notation is as defined in the main text. This quantity K is to be compared with the cloud–base mass flux, which is defined by

$$M_b = \rho_b \sigma_b w_b. \tag{A.3}$$

In order to relate the vertically–integrated convective kinetic energy, K, with the convective kinetic energy density, k, we normalize the former using

cloud–base values, σ_b and ρ_b, we normalize the updraft velocity with the characteristic velocity scaling for k, and we measure the vertical scale of convection by $h = z_T - z_B$. As a result,

$$K = 2\rho_b \sigma_b h k \int_0^1 \frac{\sigma}{\sigma_b} \frac{\rho}{\rho_b} \left(\frac{w}{w_{\text{char}}} \right)^2 d(z/h). \tag{A.4}$$

The integral now depends on dimensionless vertical profiles only and we can denote its value as ζ, which is assumed to take a fixed value for some suitable choice of w_{char}.

Hence, with the use of Eqs. A.1 and A.3, we can write

$$K = \zeta \frac{w_{\text{char}}^2 h M_B}{w_b}. \tag{A.5}$$

Now we must address the issue of the characteristic velocity scale w_{char}. It is immediately clear that the choice of this scale, and its dependence (if any) on the cloud-base mass flux will determine a suitable choice for p in Eq. 3.1.3. In other words $p = 2$ is *not demanded* by a dimensional analysis. Rather a choice for p indicated by dimensional analysis can only be discussed after one has introduced and justified physical assumptions to obtain the scale w_{char}. Some specific examples are discussed below.

1. As a trivial example we could set $w_{\text{char}} \sim L_v^{1/2}$ where L_v is the latent heat of vaporization. It must be stressed that we do not believe this scaling to be physically appropriate but clearly L_v is a relevant quantity for moist convection and on dimensional grounds alone the scaling cannot be held objectionable. In this case we might then choose $p = 1$ if we believe that h/w_b can be treated as constant, or $p = 0$ if we believe that $h\rho_b\sigma_b$ can be treated as constant.

2. A more reasonable possibility is to choose $w_{\rm char} \sim w_b$ so that w_b is the only velocity scale involved. In that case $K \sim \rho_b h \sigma_b w_b^2$. This is consistent with $p = 2$ in Eq. 3.1.3 if $h/\rho_b\sigma_b$ can be treated as constant for a given convection type. However, we argued in Plant and Yano (2012a) that this cannot be strictly true, because numerical results show that σ_b does indeed change with a change of M_b. In particular, if changes of M_b are dominated by those in σ_b rather than those in w_b (which we argued was a better interpretation of the numerical results), then we may set $p = 1$ by treating hw_b/ρ_b as constant. Thus, we see that the apparent inconsistency of Eq. 3.1.3 with the dimensional analysis stems from the fact that nondimensional variables such as σ_b may play a leading role.

3. Other velocity scales for moist convection have been proposed. For example, Grant and Brown (1999); Grant and Lock (2004) considered a velocity scale based on CAPE,

$$w_{\rm cp} = \sqrt{\rm CAPE}, \tag{A.6}$$

and a convective velocity scale w^* defined by

$$w^* = \left({\rm CAPE} \frac{M_b}{\rho_b} h \right)^{1/3}. \tag{A.7}$$

This latter scale is obtained by equating the generation and dissipation rates of turbulent kinetic energy and scaling these as ${\rm CAPE}\, M_b$ and $\rho_b w^{*3}/h$ respectively. Grant and Brown (1999) in their Figure 4 showed results for scaling the convective-core contribution to kinetic energy from their simulations for shallow convection. The results show that both scales are effective at collapsing the curves, although the latter is

perhaps somewhat better and is the one that is consistent with their physical arguments.

If we take $w_{\rm char} \sim w_{\rm cp}$ this would suggest taking $p = 1$ if CAPE h/w_b is treated as constant or else $p = 0$ if CAPE $h\rho_b\sigma_b$ is treated as constant. On the other hand, if we take $w_{\rm char} \sim w^*$ then this would suggest taking $p = 5/3$ if $({\rm CAPE}/\rho_b)^{2/3}(h^{5/3}/w_b)$ can be treated as constant or $p = 2/3$ if ${\rm CAPE}^{2/3}h^{5/3}\rho_b^{1/3}\sigma_b$ can be treated as constant. Of course, it must be remembered that the velocity scale w^* is based on a different assumption by Grant and Brown (1999) for the form of the dissipation rate compared to that in the main text.

References

Arakawa, A., and W. H. Schubert, 1974: Interaction of a cumulus cloud ensemble with the large-scale environment, Part I. *J. Atmos. Sci.*, **31**, 674–701.

Bechtold, P., J.-P. Chaboureau, A. Beljaars, A. Betts, M. Kohler, M. Miller, and J.-L. Redelsperger, 2004: The simulation of the diurnal cycle of convective precipitation over land in a global model. *Quart. J. Roy. Meteor. Soc.*, **139**, 3119–3137.

Benedict, J. J., and D. A. Randall, 2007: Observed characteristics of the MJO relative to maximum rainfall. *J. Atmos. Sci.*, **64**, 2332–2354.

Betts, A. K., 1997: Trade cumulus: observations and modelling. In: *The Physics and Parameterization of Moist Atmospheric Convection*, Kluwer Academic Publ., 99–126.

Emanuel, K. A., and M. Bister, 1996: Moist convective velocity and buoyancy scales. *J. Atmos. Sci.*, **53**, 3276–3285.

Emanuel, K. A., J. D. Neelin, and C. S. Bretherton, 1994: On large–scale circulation in convective atmospheres. *Quart. J. Roy. Meteor. Soc.*, **120**, 1111–1143.

Grant, A. L. M. and A. R. Brown, 1999: A similarity hypothesis for shallow-cumulus transports. *Quart. J. Roy. Meteor. Soc.*, **125**, 1913–1936.

Grant, A. L. M. and A. P. Lock, 2004: The turbulent kinetic energy budget for shallow cumulus convection. *Quart. J. Roy. Meteor. Soc.*, **130**, 401–422.

Grabowski, W. W., P. Bechtold, A. Cheng, R. Forbes, C. Halliwell, M. Khairoutdinov, S. Lang, T. Nasuno, J. Petch, W.-K. Tao, R. Wong, X. Wu and K.-M. Xu, 2006: Daytime convective development over land: A model intercomparison based on LBA observations. *Quart. J. Roy. Meteor. Soc.*, **132**, 317–344.

Guichard F., J. C. Petch, J. L. Redelsperger, P. Bechtold, J.–P. Chaboureau, S. Cheinet, W. Grabowski, H. Grenier, C. G. Jones, M. Kohler, J.–M. Piriou, R. Tailleux, and M. Tomasini, 2004: Modelling the diurnal cycle of deep precipitating convection over land with cloud-resolving models and single-column models. *Quart. J. Roy. Meteor. Soc.*, **604**, 3139–3172.

Hohenegger, C., and C. S. Bretherton, 2011: Simulating deep convection with a shallow convection scheme. *Atmos. Chem. Phys.*, **11**, 8385–8430.

Holtslag, A. A. M., and B. A. Boville, 1993: Local versus nonlocal boundary–layer diffusion in a global climate model. *J. Climate*, **6**, 1825–1842.

Houze, R. A., Jr., and A. K. Betts, 1981: Convection in GATE, *Rev. Geophys. Space Phys.*, **19**, 541-576.

Johnson, R. H., Rickenbach, T. M., Rutledge, S. A., Ciesielski, P. E., and Schubert, W. H., 1999: Trimodal characteristics of tropical convection. *J. Climate*, **12**, 2397–2418.

Köller, M., M. Ahlgrimm, and A. Beljaars, 2011: Unified treatment of dry convective and stratocumulus–topped boundary layers in the ECMWF model. *Quart. J. Roy. Meteor. Soc.*, **137**, 43–57.

Lock, A. P., 1998: The parameterization of entrainment in cloudy boundary layers. *Quart. J. Roy. Meteor. Soc.*, **124**, 2729–2753.

Lock, A. P., A. R. Brown, M. R. Bush, G. M. Martin, and R. N. B. Smith, 2000: A new boundary layer mixing scheme. Part I: Scheme description and single–column model tests. *Mon. Wea. Rev.*, **128**, 3187–3199.

Mapes, B. E., and R. Neale, 2011: Parameterizing convective organization to escape the entrainment dilemma. *J. Adv. Model Earth System*, **3**, doi:10.1029/2011MS000042.

Moeng, C.–H., 1998: Stratocumulus–topped atmospheric planetary boundary layer. In: *Buoyant Convection in Geophysical Flows*, E. J. Plate, E. E. Fedorovich, D. X. Viegas, and J. C. Wyngaard, Eds., Kulwer Academic Publ., 421–440.

Neggers, R., M. Köller, and A. Beljaars, 2009: A dual mass flux framework for boundary–layer convection. Part I: Transport. *J. Atmos. Sci.*, **66**, 1465–1487.

Pan, D.-M., and D. A. Randall, 1998: A cumulus parameterization with prognostic closure, *Quart. J. Roy. Meteor. Soc.*, **124**, 949–981.

Parodi, A., and K. Emanuel, 2009: A theory for buoyancy and velocity scales in

deep moist convection. *J. Atmos. Sci.*, **66**, 3449–3463.

Parsons, D. B., K. Yoneyama, and J.–L. Redelsperger, 2000: The evolution of the tropical western Pacific atmosphere–ocean system following the arrival of a dry intrusion. *Quart. J. Roy. Meteor. Soc.*, **126**, 517–548.

Plant, R. S., 2012: A new modelling framework for statistical cumulus dynamics. *Phil. Trans. Roy. Soc.*, **A370**, 1041–1060.

Randall, D. A., and D.-M. Pan, 1993: Implementation of the Arakawa-Schubert cumulus parameterization with a prognostic closure. In: *The Representation of Cumulus Convection in Numerical Models*, K. A. Emanuel and D. J. Raymond (Eds.), Meteorological Monographs **46**, Amer. Meteor. Soc., 137–144.

Riehl, H., C. Yeh, J. S. Malkus, and N. E. LaSeur, 1951: The north–east trade of the Pacific Ocean. *Quart. J. Roy. Meteor. Soc.*, **77**, 598–626.

Redelsperger, J.–L., 1997: The mesoscale organization of deep convection. In: *The Physics and Parameterization of Moist Atmospheric Convection*, R. K. Smith (Ed.), Kluwer Academic Publ., 59–98.

Riehl, H., and J. S. Malkus, 1958: On the heat balance in the equatorial trough zone. *Geophysica*, **6**, 503–538.

Shutts, G. J., and M. E. B. Gray, 1999: Numerical simulations of convective equilibrium under prescribed forcing. *Quart. J. Roy. Meteor. Soc.*, **125**, 2767–2787.

Stevens, B., 2005: Atmospheric moist convection. *Ann. Rev. Earth Planet. Sci.*, **33**, 605–643.

Tiedtke, M., 1989: A comprehensive mass flux scheme of cumulus parameterization in large–scale models. *Mon. Wea. Rev.*, **117**, 1779–1800.

Tung, W. W., C. Lin, B. Chen, M. Yanai, and A. Arakawa, 1999: Basic mode of cumulus heating and drying observed during TOGA–COARE IOP. *Geophys. Res. Lett.*, **26**, 117–120.

Wyant, M. C., C. S. Bretherton, A. Chlond, B. M. Griffin, H. Kitagawa, C.–L. Lappen, V. E. Larson, A. Lock, S. Park, S. R. de Roode, J. Uchida, M. Zhao, A. S. Ackerman, 2007: A single–column model intercomparison of a heavily drizzling stratocumulus–topped boundary layer. *J. Geophys. Res.*, **112**, D24204, doi:10.1029/2007JD008536.

Yano J.-I., M. Bister, Z. Fuchs, L. Gerard, V. Phillips, S. Barkidija, and J.-M. Piriou, 2012: Phenomenology of convection-parameterization closure. *Atmos. Chem. Phys. Discuss.*, **12**, 25743–25789.

Yano, J.-I., and R. S. Plant, 2012a: Finite departure from convective quasi-equilibrium: Periodic cycle and discharge-recharge mechanism. *Quart. J. Roy. Meteor. Soc.*, **138**, 626–637.

Yano, J.-I., and R. S. Plant 2012b: Interactions between shallow and deep convection under a finite departure from convective quasi–equilibrium. *J. Atmos. Sci.*, **69**, 3463–3470.

Yano, J.-I., and R. S. Plant, 2012c: Convective quasi–equilibrium. *Rev. Geophys.*, **50**, RG4004, doi:10.1029/2011RG000378.